

1 **New loci and candidate genes in spring two-rowed barley detected
2 through meta-analysis of a field trial European network**

3 **Francesc Montardit-Tarda¹, Ana M Casas¹, William TB Thomas², Florian
4 Schnaithmann³, Rajiv Sharma^{4,5}, Salar Shaaf^{4,6}, Chiara Campoli², Joanne Russell², Luke
5 Ramsay², Stefano Delbono⁷, Marko Jääskeläinen^{8,9}, Maitry Paul^{8,9}, Frederick L
6 Stoddard^{9,10}, Andrea Visioni¹¹, Andrew J Flavell¹², Klaus Pillen³, Benjamin Kilian^{4,13},
7 Andreas Graner⁴, Laura Rossini⁶, Robbie Waugh², Luigi Cattivelli⁷, Alan H
8 Schulman^{8,9,10}, Alessandro Tondelli⁷, Ernesto Igartua^{1,*}**

9 ¹Estación Experimental de Aula Dei – Consejo Superior de Investigaciones Científicas
10 (EEAD-CSIC), Avenida Montañana 1005, 500059, Zaragoza, España

11 ²James Hutton Institute, Errol Road, Invergowrie, Dundee DD2 5DA, United Kingdom

12 ³Martin-Luther-Univ. Halle-Wittenberg, Betty-Heimann-Str. 3, 06120 Halle (Saale),
13 Germany

14 ⁴Leibniz Institute of Plant Genetics and Crop Plant Research (IPK), Corrensstrasse 3,
15 06466 Gatersleben, Germany

16 ⁵Scotland's Rural College, Peter Wilson Building, The King's Buildings, West Mains Road,
17 Edinburgh EH9 3JG, United Kingdom

18 ⁶Università degli Studi di Milano, Via Celoria 2, 20133 Milano, Italy

19 ⁷Council for Agricultural Research and Economics (CREA), Research Centre for Genomics
20 and Bioinformatics, Via San Protaso 302, 29017 Fiorenzuola d'Arda, Italy

21 ⁸Institute of Biotechnology, University of Helsinki, FI-00014 Helsinki, Finland

22 ⁹Viikki Plant Sciences Centre, University of Helsinki, FI-00014 Helsinki, Finland

23 ¹⁰Natural Resources Institute Finland (LUKE), FI-00014 Helsinki, Finland

24 ¹¹International Center for Agricultural Research in the Dry Areas (ICARDA), Rabat 10100,
25 Morocco

26 ¹²Dundee University at SCRI, Invergowrie, Dundee DD2 5DA, United Kingdom

27 ¹³Global Crop Diversity Trust, Platz Der Vereinten Nationen 7, 53113 Bonn, Germany

28 *Correspondence: igartua@eead.csic.es

29

30 **Short running title: Meta-analysis of agronomic traits in spring barley**

31

32 **Highlight**

33 A dense genome-wide meta-analysis provides new QTLs, reveals breeding history trends
34 and identifies new candidate genes for yield, plant height, grain weight and heading time
35 of spring barley.

36 **Abstract**

37 This study contributes new knowledge on quantitative trait loci (QTLs) and candidate
38 genes for adaptive traits and yield in two-rowed spring barley. A meta-analysis of a
39 network of field trials, varying in latitude and sowing date, with 151 cultivars across
40 several European countries, increased QTL detection power compared to single-trial
41 analyses. The traits analysed were heading date (HD), plant height (PH), thousand-grain
42 weight (TGW), and grain yield (GY). Breaking down the analysis by the main genotype-
43 by-environment trends revealed QTLs and candidate genes specific to conditions like
44 sowing date and latitude. A historical look on the evolution of QTL frequencies revealed
45 that early selection focused on PH and TGW, likely due to their high heritability. GY
46 selection occurred later, facilitated by reduced variance in other traits. The study
47 observed that favourable alleles for plant height were often fixed before those for grain
48 yield and TGW. Some regions showed linkage in repulsion, suggesting targets for future
49 breeding. Several candidate genes were identified, including known genes and new
50 candidates based on orthology with rice. Remarkably, the *deficiens* allele of gene *Vrs1*,
51 appears associated to higher GY. These findings provide valuable insights for barley
52 breeders aiming to improve yield, and other agronomic traits.

53 **Keywords:** agronomic traits, barley, breeding history, GWAS, meta-analysis, *Vrs1*

54 Introduction

55 Barley (*Hordeum vulgare* L.) is the fourth-ranking cereal in the world, and one of the
56 most important crops in Europe, in terms of cultivation area and economic relevance
57 (Dawson et al., 2015, Looseley et al., 2020). In Europe, barley has been the subject of
58 intensive breeding for over 100 years. Competitive breeding in the spring two-rowed
59 pool, with thorough use of the traditional “cross the best with the best and hope for the
60 best” strategy has increased concerns about possible genetic erosion in the cultivated
61 germplasm pool. This process has led to the preferential selection of some genomic
62 regions, and to an overall decrease in genetic diversity, particularly in the spring barley
63 pool (Kolodinska Brantestam et al., 2004; Dziurdziak et al., 2022; Schmidt et al., 2023).
64 Indeed, Tondelli et al. (2013) detected signs of extinction of diversity in some genomic
65 regions. Intensive breeding activities usually produce, inadvertently or consciously,
66 fixation of alleles with large effects on important target traits. However, genetic
67 variation is still present (Tondelli et al., 2013), although finding QTLs, even with small
68 effects, becomes harder. One way to detect minor QTLs is by relying on extensive
69 phenotyping and meta-analysis (Muñoz-Amatriaín et al., 2020). In many European
70 regions, barley with spring growth habit is sown between February and May, to avoid
71 harsh winters. This is mandatory in Nordic countries and other European areas with
72 harsh winters, particularly in Eastern Europe, but cultivation of spring-type barley occurs
73 throughout Europe. Its relevance is increasing for two reasons. On the one hand,
74 increasing winter temperatures allow its cultivation in areas of Europe (like Germany,
75 Italy, Spain, or Switzerland) where winter barley and autumn/winter sowings were
76 prevalent. On the other hand, the main economic boost for barley breeding in Europe
77 has been, and still is, malting quality, a sector largely dominated by spring two-rowed
78 types, consequently, breeding efforts have been particularly intense within this pool,
79 giving rise to malting cultivars as productive as the best feed barleys.

80 Genome-wide Association (GWA) studies have been widely used in barley to find
81 genomic regions of interest for a large variety of agronomic characters (Igartua et al.,
82 2019; Thomas, 2020). In some cases, candidate genes were identified and validated,
83 making for straightforward breeding. Even so, this is only possible when large diversity
84 panels are available, combined with enough marker density. Marker density provided
85 by the 50k SNP chip (Bayer et al., 2017) gives the opportunity to search for candidate
86 genes in association studies. In narrow germplasm sets, linkage disequilibrium (LD)
87 should be high, hence relatively low marker density is sufficient to pinpoint QTL regions
88 in GWA studies (GWAS). However, to differentiate cultivars that are very close, and be

89 able to track alleles of candidate genes, higher marker densities eventually are needed.
90 This is likely the case of the cultivated spring two-rowed barley pool. Dense genotyping
91 can be achieved using exome capture data, which is available in barley (Mascher et al.,
92 2013; Russell et al., 2016; Chen et al., 2022). Another aspect which has not been fully
93 exploited in GWA is the information from multi-trial studies. With few exceptions (for
94 instance Bustos-Korts et al., 2019), these are analysed as the mean of all trials, or by
95 identifying the intersection of associated markers between single-trials analyses. These
96 methods do not make full use of the potential of independent effects tested in multiple
97 sites to detect QTLs (Muñoz-Amatriain et al., 2020).

98 This study aims at finding new QTLs for relevant agronomic traits in spring two-rowed
99 barley cultivars, and at indicating new candidate genes that may become new targets
100 for barley breeding in Europe.

101 **Materials and methods**

102 **Plant material**

103 A collection of 164 spring two-rowed cultivars was tested in the framework of the
104 international projects EXBARDIV ([http://pgrc.ipk-
105 gatersleben.de/barleynet/projects_exbardiv.php](http://pgrc.ipk-gatersleben.de/barleynet/projects_exbardiv.php)) and CLIMBAR ([https://project-
106 wheel.faccejpi.net/climbar/](https://project-wheel.faccejpi.net/climbar/)). The two projects included extensive sets of genotypes, but
107 only spring two-rowed cultivars common to both projects were kept for this study. A
108 principal component analysis for marker data was carried out with the *SNPRelate*
109 package (Zheng et al., 2012) in R (R Core Team, 2024). Cultivars clearly outside the
110 principal cloud of points were filtered out (Fig. S1). Discarded cultivars either originated
111 in southern Europe (likely representing distinct germplasm pools) or had introgressions
112 from exotic parents. A total of 151 cultivars that did not show a clear population
113 structure were kept for further analyses (Table S1).

114 **Phenotypic evaluation, curation and analysis**

115 Field trials were carried out in 2009 and 2010 within the EXBARDIV project, and in 2016
116 and 2017 in the framework of the CLIMBAR project, in the United Kingdom, Finland,
117 Germany, Italy, Spain and Morocco (Table 1, Table S2). All trials consisted of plots of four
118 to eight rows, 2-3 m long, and 1-1.5 m wide, in two replicates, following alpha-lattice
119 designs, with plots managed according to local practices for sowing rate and chemical
120 inputs. Flowering time (HD, days from sowing to appearance of the spike out of the flag

121 leaf sheath, Z55, according to Zadoks et al. 1974), plant height (PH, cm, length from the
122 ground to the tip of the spike, without awns, average of five plants), grain yield after
123 combine harvest (GY), and thousand grain weight (TGW) were recorded. Raw
124 phenotypic data from EXBARDIV were retrieved for the 2009 and 2010 seasons, partially
125 reported in Xu et al. (2018). Phenotypic data were curated for outlier data. Two trials
126 (MAR17 and DE2-10) were fully discarded due either to consistently low correlation
127 coefficients with the rest (Fig. S2) or to low overall data quality. Data from 16 trials were
128 kept for HD, PH and GY, while TGW was recorded from 15 trials only.

129 Best linear unbiased estimators (BLUEs) were calculated with Genstat 20 (VSN
130 International, 2022). In each trial, the best spatial correction model was used, with the
131 simplest model being a randomized complete block design; the full model including
132 replicates, autoregressive order 1 in rows and columns, and additional contributions
133 from significant random row and column factors (Table S2). Chi-square tests were
134 performed for models differing by a single factor. The most parsimonious model for each
135 trait was chosen, the last in which the inclusion of a spatial correction factor improved
136 the model significantly. If a given cultivar had missing data in three or less trials, its
137 phenotype was imputed with the value corresponding to the percentile of that trait for
138 the missing cultivar in the average of the remaining trials (21, 21, 27 and 17 imputed
139 values for HD, PH, GY and TGW, respectively).

140 An additive main effects and multiplicative interaction analysis (AMMI) was done for
141 each trait with Genstat 20 (VSN International, 2022). These analyses were used to cluster
142 the trials into mega-environments, following the main direction of genotype by
143 environment interaction (GEI) per trait.

144 **Genotyping**

145 The lines were genotyped with the 50k Illumina Infinium SNP Array (Bayer et al., 2017).
146 Missing data were imputed with Beagle 5.0 (Browning et al., 2018), as described in
147 Bretani et al. (2022). After imputation, 40639 markers remained. For further analysis,
148 markers with a minor allele frequency equal to or higher than 0.05 were kept (28988
149 markers). Physical positions of markers were retrieved from both MorexV1 (Mascher et
150 al., 2017) and MorexV3 (Mascher et al., 2021). Additional genotyping for flowering time
151 genes and *Vrs1* (main gene determining spike type) was performed for all lines, with
152 specific markers developed as described in Table S1.

153 **Genome-Wide Association Analysis and meta-analysis**

154 Association analyses at the single trial level were carried out for all phenotypes and trials
155 using the mixed linear model (MLM) implemented in the GAPIT package (Wang and
156 Zhang, 2021) in R (R Core Team, 2024), with a genomic kinship matrix for adjustment of
157 relatedness, calculated with a randomly selected set of 10% of markers (Fig. S3).

158 The results of a single trial GWA per trait were meta-analysed with the software METAL
159 (Willer et al., 2010), using the sample size strategy, for the whole set of trials, and for
160 the best grouping of trials indicated by the AMMI analysis. For grain yield, ITA16 and
161 ITA17 were discarded for meta-analysis due to the high dispersion within each trial. A
162 meta-GWA threshold was calculated as the minimum p -value detected by 1000
163 meta-analysis of 1000 permutations per trial, for each phenotype and combination of
164 trials. Markers with a higher $-\log_{10}(p\text{-val})$ than the threshold were declared as a marker-
165 trait association (MTA). Neighbouring MTAs were grouped into single QTL with two
166 different criteria. First, MTAs from the same chromosome were grouped according to a
167 cluster analysis, as in Looseley et al. (2020). The marker with the largest association per
168 QTL was declared as flag marker. Then, flag markers from the same chromosome, which
169 were in the same LD block (detailed below), were merged.

170 **Linkage disequilibrium analysis**

171 A basal genomic LD threshold was computed. This threshold was estimated as the
172 square of the 95th percentile of the distribution of unlinked r^2 values (square root
173 transformed), as in Breseghello and Sorrells (2006). This distribution was fitted with the
174 values of the interchromosomal r^2 between 200 random markers per chromosome,
175 discounting the population structure using the $r2v$ parameter, using the R package
176 *LDcorSV* (Mangin et al., 2012), which considers kinship relatedness. For each
177 chromosome, intrachromosomal LD block size was calculated using $r2v$, for pairwise LD
178 values between 500 random markers per chromosome. Chromosomal LD decay was
179 calculated as the point where a loess regression intercepted with the basal genomic LD,
180 using R package *fitdistrplus* (Delignette-Muller and Dutang, 2015); this procedure served
181 to merge the flag markers of several MTAs into a single QTL.

182 To search for candidate genes, the confidence region for each QTL was calculated. Local
183 LD decay around each flag marker was estimated fitting a loess regression to the
184 pairwise LD values from the closest 400 markers. The confidence region was defined as
185 the distance from the flag marker to the point where the loess curve decreased to the
186 basal genomic LD threshold. When the loess curves did not converge, the chromosomal
187 LD was used instead to declare confidence intervals.

188 **Meta-analysis multilocus model**

189 The markers found in the meta-analysis may still present some multicollinearity. To
190 reduce it, sequential multivariate analyses of variance were carried out for each trait,
191 with package *car* (Fox and Weisberg, 2019). The flag markers were introduced as
192 independent variables, and the genotypic values for each trial were the dependent
193 variables. Markers were introduced sequentially at each step, keeping in the model the
194 most significant one at each round. The final model summarizes the set of markers most
195 likely having a combined independent effect for all trials, on each trait.

196 **GWA enrichment with exome capture markers**

197 Markers based on exome capture (EC) (Chen et al., 2022) were used for the refinement
198 of peak regions found with 50k markers. For each QTL, all available markers (50k + EC
199 markers) within its local LD block were retrieved and a single-trial GWA and its meta-
200 analysis were run again. Exome capture markers with higher $-\log_{10}(p\text{-values})$ than that
201 of the flag marker were considered indicators of a possible candidate gene. Relevant
202 annotations of homologs from other species and gene expression (Milne et al., 2021; Li
203 et al., 2023) in tissues related to the phenotype were considered as additional pointers
204 for possible candidate genes.

205 Homologues of the candidate genes from *Arabidopsis thaliana*, rice, and wheat were
206 identified with protein BLAST in order to gather functional information using Ensembl
207 Plants (Yates et al., 2022). Only the top homologue with an identity above 80% was
208 considered. Orthologues of *Oryza sativa subsp. japonica* of each candidate gene were
209 identified with Ensembl Plants. FunRiceGenes (Huang et al., 2022) was used to check if
210 a rice orthologue was a trait-related gene.

211 **Allele frequency shifts over time of cultivar release**

212 The genotypic panel used is representative of the progression of spring barley breeding
213 in Europe. The wide range in the cultivars' year of release enables tracking of the fate of
214 QTLs in parallel with the history of European spring barley breeding. The cultivars were
215 grouped by year of release into four groups, with the number of cultivars in parentheses:
216 1920-1959 (n = 18), 1960-1979 (38), 1980-1999 (69) and 2000- (29), respectively. Mean
217 allele frequencies of 250 rolling windows per chromosome were calculated for the four
218 groups of cultivars. MetaQTLs allele frequencies were also calculated for the same four
219 classes, to describe any trends likely due to breeding. Allele frequency shifts of

220 metaQTLs, and genome-wide rolling windows, were determined as the difference
221 between the allele frequencies of the oldest and most recent group of cultivars.

222 **Results**

223 **Field trial results**

224 The field trials represented a varied range of latitudes, climates, and edaphic and
225 agronomic conditions. Accordingly, grain yields were highly variable, between 2.8 and
226 8.0 t ha⁻¹, with an overall yield of 4.9 t ha⁻¹. Autumn- or winter-sown trials in Spain and
227 Morocco showed the lowest yields, while trials autumn-sown in Italy and spring-sown
228 trials at northern latitudes were more productive (Table 1, Fig. S4). The largest variation
229 in days from sowing to heading was mainly caused by sowing date. The trials that were
230 autumn-sown in Italy or Spain, as well as the winter-sown trial in Morocco, experienced
231 longer cycles, followed by the late-winter-sown trials in Italy (ITA09 and ITA10, sown in
232 February and early March), and by all the spring-sown trials. Among the latter, Scottish
233 trials showed longer seasons than German and Finnish trials. Within sowing dates, those
234 differences in cycle lengths were probably caused by different rates of accumulation of
235 growing degree days. Plant height also varied widely between trial means, from 52 to
236 90 cm, suggesting a large variability in water availability during the stem elongation
237 phase. Thousand-grain weight (TGW) varied between 33 g, for some southern locations,
238 to 51 g in the Scottish trials, indicating highly variable grain filling conditions. Grain yield
239 trial means showed a tight correlation of 0.84 with plant height (a surrogate of biomass)
240 and a moderate correlation with TGW (0.60), indicating the importance of the biomass
241 formation phase, throughout the entire season, and of the conditions prevalent during
242 grain filling for grain yield build-up (Fig. S5).

243 For all the traits, both the genotypic and genotype by environment (G x E) interaction
244 effects were significant. In general, G x E was more relevant for GY or TGW than for HD
245 or PH but, in all cases, the genotypic sum of squares was much larger. G x E patterns
246 revealed by the AMMI analysis were different for each trait. For grain yield, most trials
247 formed a tight cloud, except those of ITA16 and ITA17, both being trials with high yields
248 having a large effect on overall G x E variance (Table 2, Fig. S6). For heading date (Fig. 1),
249 the first principal component reflected mainly a difference between sowing dates, with
250 autumn-sown (ESP16, ESP17, ITA16, ITA17) or winter-sown trials (MAR16) showing large
251 positive loadings, spring-sown ones (DE1-09, DE1-10, DE2-09, GBR09, GBR10, GBR16,
252 GBR17, FIN16, FIN17) placed opposite to them, and intermediate-sowing dates (ITA09

253 and ITA10) in a halfway position. ITA09 and ITA10 were, however, classified as spring
254 trials for meta-analysis. The first principal component explained a large proportion of G
255 x E, and was strongly influenced by the differential behaviour of Nordic cultivars Mona
256 and Saana. These cultivars were relatively later in the northernmost environments, and
257 very early in the autumn-sown trials. This was also evidenced by the comparison of the
258 differences between heading date of these cultivars and the overall mean at each trial
259 (Fig. S7). The distribution of trials over the first component for plant height showed a
260 geographic pattern, with most southern environments (Italy, Morocco and Spain) on one
261 side of the first axis, and most northern towards the opposite side (Finland, Germany
262 and the United Kingdom). For TGW, the unique behaviour of ITA16 was the main cause
263 of the very large first principal component.

264 **QTL analysis at single environments**

265 GWA analyses of the four phenotypic traits at the single-trial level produced relatively
266 weak associations. For grain yield, only two MTAs were detected above a Bonferroni
267 threshold of $P<0.05$, while 20 MTAs were detected for heading date and none both for
268 plant height and for thousand grain weight. Both MTAs of GY were detected from ITA10;
269 the 20 MTAs for HD were from ESP16. Lowering the threshold to a more liberal
270 $p<0.0001$, commonly used in GWA studies, still detected 125 MTAs for grain yield, 96
271 MTAs for heading date, 54 MTAs for plant height, and 10 MTAs for TGW (Table S3). Some
272 regions with common QTLs across trials were suggested but, overall, the number and
273 strength of associations found was low.

274 **QTL meta-analysis**

275 The meta-analyses amplified the association signals, based on the relevance of p -values
276 and the commonality in the direction of the effects sign across trials. The results were
277 analysed using a stringent threshold based on permutations. Many SNPs had
278 associations above that threshold. Some markers clearly indicated the same
279 chromosome region. Associated markers were merged into QTLs, combining several
280 criteria. All associated markers in a chromosome were subjected to cluster analysis, as
281 in Looseley et al. (2020), suggesting groups likely belonging to the same QTL. The local
282 LD decay (and chromosomal LD decay, if local LD was indeterminate), helped to delimit
283 the QTLs on each chromosome. This process resulted in the detection of 23 QTLs for
284 heading date, 29 for plant height, 11 for grain yield, and 27 for thousand grain weight
285 (Table 3, Fig.2, Fig. S8). These numbers are rather high, because of the detection of QTLs
286 having minor effects, which are usually not found in studies of smaller scale. The meta-

287 analysis tends to identify MTAs that show the same sign across all trials. For this reason,
288 it is not expected that it will capture qualitative QTL-by-environment interactions, if
289 these exist. Therefore, most QTLs were rather consistent across trials (Table 3).
290 However, some patterns of interaction were evident for a few QTLs, particularly for
291 heading date. The differences in significance between the autumn- and spring-sown
292 trials were large in some cases. The QTLs for HD5 (Fig. 3), HD6, and HD8 were much
293 more significant in spring than in autumn trials. Conversely, HD21 was relatively more
294 important in autumn-sown trials. There was a single QTL detected in the analyses of HD
295 split by sowing time that was not detected in the global analysis. HDA1, on 1H, was
296 significant only in the autumn-sown trials, indicating a marked QTL-by-environment
297 interaction, possibly of qualitative nature, at this locus. The QTL-by-environment
298 interaction was less evident for plant height (Table 3), as shown by PH14 (Fig. 3).

299 Multilocus models derived from sequential MANOVA analyses were used to identify the
300 best subset of significant QTLs that jointly explained each trait. All QTLs included in the
301 models were significant for $P < 0.05$ or less and had partial Eta squared (η_p^2) above 0.14.
302 This value is commonly used as threshold to declare the influence of independent
303 factors on the dependent variables. These joint models explained around 16% of
304 phenotypic variance for HD, TGW, and GY, and 33% for PH (Table 4). The QTLs retained
305 in the models had a rather small effect, explaining from 1.08 up to 6.07 percent of the
306 variance of the traits: from 0.14 to 0.33 t ha⁻¹ (averaged across all environments) for GY,
307 from 0.7 to 1.9 days for HD, 1.4 to 2.7 cm for PH, and 0.6 to 1.3 g for TGW. The QTLs
308 explaining more than 5% of the variance of the trait were PH28, on 7H (2.5 cm), and
309 GY2, on 1H (5.08%, 0.28 t ha⁻¹).

310 The intervals for confidence regions of the QTLs were wide, with a mean size of 25.95
311 Mb. Regions ranged from 1.23 Mb to 349.45 Mb, illustrating just how unevenly
312 distributed is LD in spring barley germplasm. Moreover, two regions of nearly 350 Mb
313 were identified on chromosome 7H, most likely related to an inversion of 141 Mb
314 (Jayakodi et al., 2020) that already has been identified in some cultivars included in our
315 association panel. There was overlap between the confidence intervals for QTLs of
316 different traits, as indicated in Table S4. The region of TGW15-PH19 could represent the
317 same QTL with pleiotropic effects. Some grain yield QTLs overlap with plant height
318 (PH4), and thousand grain weight (TGW5, TGW25, TGW26, and TGW27). Other QTLs
319 were linked to some extent, which may have implications for their management in
320 breeding.

321 Temporal variation in traits and QTL allelic frequencies

322 The classification of cultivars into four classes, according to the year of release, revealed
323 salient trait and QTL trends resulting from breeding efforts and preferences. Plant height
324 and thousand-grain weight presented marked trends towards reduced (PH) or increased
325 (TGW) values through the years, in accordance with the expected outcome from
326 breeding programs (Fig. 4) and these traits' heritability (Table 1). The trends were highly
327 consistent across environments (Fig. S4). For grain yield, the increase over time was less
328 marked, except in Scotland. In general, the largest yield improvement was observed for
329 the most modern cultivars compared to earlier ones. There were no marked historic
330 trends regarding heading date. The only remarkable feature was that the most modern
331 class of cultivars was always the earliest in all spring-grown trials, whereas this
332 difference was not observed in the autumn-sown trials, hinting at the occurrence of a
333 possible genotype-by-environment interaction.

334 Regarding allelic frequencies for QTLs over time, some QTLs followed the general trend
335 for their trait, while others showed no apparent response. For PH, the height-increasing
336 alleles of eight QTLs were already at low frequencies in the old cultivars; these remained
337 low thereafter. Five QTLs (PH10, PH11, PH17, PH24, PH26) seemed not to be affected
338 by selection, keeping high to very high frequencies of height-increasing alleles, whereas
339 11 QTLs exhibited marked increases in the frequency of height-reducing alleles
340 (coloured lines, Fig. 5). For TGW (Fig. S9), the situation was similar, but with fewer QTLs
341 apparently affected by selection. Five QTLs (TGW2, TGW5, TGW6, TGW11, TGW12)
342 showed high frequencies of grain-weight-increasing alleles already in the oldest cultivar
343 class, increasing slightly to almost fixation in the most modern class. The frequencies of
344 another five QTLs (TGW7, TGW14, TGW18, TGW20, TGW26) for higher grain weight
345 approximately doubled over time, i.e., were apparently favoured by selection. For
346 another 17 QTLs, frequencies of favourable alleles varied between medium to low, with
347 little or no response to selection. For GY, the frequency shifts of several QTLs occurred
348 only in the most recent groups of cultivars. An exception was GY7, which was the QTL
349 having the largest frequency change over time, considering all four analysed traits. For
350 HD (Fig. S9), there were three QTLs that were apparently affected by selection (HD5,
351 HD6 and HD8). These QTLs suffered some selection towards earliness. It is remarkable
352 that these three QTLs were detected in the spring-sown trials, yet not in the
353 autumn-sown ones (Table 3), showing the largest difference in significance between the
354 two sets of trials. They may be responsible for the increased earliness shown by the most
355 modern class of cultivars, which is seen only under spring-sown conditions.

356 At the genome level, some regions seemed preferentially targeted by selection. This was
357 examined by looking at the difference in frequencies between the oldest and newest
358 cultivar classes, calculated for the SNPs divided in 250 rolling windows (bins) per
359 chromosome for all four groups of year of release (Fig. S10). Focusing on the 1% of bins
360 with the largest frequency changes, the most visible selection footprint was in the
361 pericentromeric area of chromosome 5H (65-310 Mb), coincident with the haplotype
362 already detected by Wonneberger et al. (2023). Another narrow region in 5HL (around
363 543 Mb) showed similar allele frequency changes. Finally, a region in 4HL (510-530 Mb)
364 also showed two close, narrow peaks of very large frequency shifts over time. For all
365 traits, we have identified some QTLs apparently untouched by selection and some at
366 low frequencies in the set studied. These could be aimed at by current breeders,
367 provided they have not already been targeted by breeding in recent years and that they
368 do not convey negative pleiotropic effects.

369 **Exome capture enrichment and candidate genes**

370 The inclusion of exome capture (EC) data for the analysis of the QTLs detected provided
371 119,811 more markers. In 25 cases (31.65%), exome capture markers had equal or
372 higher association than for the 50k SNPs (Table S5); these were designated as the new
373 flag SNPs. For each QTL, a search of candidate genes for the flag markers was carried
374 out within the confidence interval regions. In some cases, flag markers were present
375 inside genes having annotations relevant for the traits considered. The EC markers
376 provided higher resolution than did SNPs from the 50k set, for example, in the region of
377 flowering time QTL HD17 on chromosome 6H. That confidence interval region harbours
378 two flowering-related genes, *HvCMF3* (Cockram et al., 2012) and *HvZTLb* (Russell et al.,
379 2016). However, the EC marker with the largest association is located inside gene model
380 HORVU.MOREX.r3.6HG0557980, annotated as the nuclear pore complex protein Nup
381 160.

382 Several plant height QTLs presented EC markers with higher associations than those of
383 markers in the 50k SNP set. PH1 showed highly associated EC markers in two different
384 genes. While the most strongly associated marker was within a low-confidence gene,
385 the second group of highly associated markers pointed to a nitrate transporter
386 (HORVU.MOREX.r3.1HG0005090), which is an ortholog of rice *OsNRT1.4* (Bucher et al.,
387 2014). PH24, which presents one of the highest associations, was within gene
388 HORVU.MOREX.r3.6HG0632820, annotated as a WRKY transcription factor-like protein.
389 The *sdw1* gene is a good candidate for QTL PH14. Mutations in this gene, a gibberellin

390 20-oxidase gene (*HvGA20ox2*), are one of the most common causes of semi-dwarfism in
391 barley. It is a multiallelic locus, with a few alleles commonly employed in barley breeding
392 to reduce plant height (Xu et al., 2017).

393 Half of the QTLs for thousand-grain weight contained interesting candidate genes,
394 indicated by a higher association of an EC marker. For TGW18, included in the
395 multivariate multilocus model, an ortholog of rice gene *OsBRXL4* was identified
396 (HORVU.MOREX.r3.5HG0535760). The EC flag maker gene for TGW27 is
397 HORVU.MOREX.r3.7HG0752360, which is a lysine-specific demethylase. Interestingly,
398 this is the same annotation of the *Vrs3* gene (Bull et al., 2017; van Esse et al., 2017) and
399 is expressed in developing inflorescences and grains. Its homologous gene in *A. thaliana*
400 is activated under dehydration stress (Huang et al., 2019). For grain yield, enrichment
401 with EC markers identified a gene coding an α -glucosidase enzyme in QTL GY5. This gene,
402 *HvAGL2* (HORVU.MOREX.r3.3HG0221900) was previously confirmed to be involved in
403 starch metabolism in developing grains in barley (Andriotis et al., 2016). The GY2
404 confidence interval includes the *HvHOX1* (*Vrs1*) gene, involved in spike-row
405 determination (Komatsuda et al., 2007). We used a specifically-designed KASP marker
406 (Table S1) to genotype the panel for the *deficiens* allele *Vrs1.t*. None of the cultivars with
407 the unfavourable allele at GY2 carried *Vrs1.t*. Out of the 15 cultivars carrying the
408 favourable allele at QTL GY2, 14 were available to phenotype and genotype. Thirteen of
409 them (all but Forum) carried the *deficiens* allele. An evaluation of the spikes of the 14
410 revealed differences in the size of the lateral spikelets. Eleven cultivars were
411 phenotypically *deficiens*, without lateral spikelets. Forum was clearly not *deficiens*,
412 genetically and phenotypically. Although Felicitas and Tocada are genetically *deficiens*,
413 both showed very small laterals spikelets (Fig. S11). These results support *Vrs1* as a
414 candidate gene for GY2.

415 **DISCUSSION**

416 The sensitivity of the meta-analysis varied among traits. Using the rather liberal
417 threshold (widely found in the literature) of $-\log_{10}(p\text{-value}) = 4$ at single-trial level, a total
418 of 96 MTAs were detected for HD, in approximately 16 regions, with no QTL detected in
419 more than three trials, while the meta-GWA allowed identification of 22 QTLs in high-
420 confidence regions for HD (reduced to eight in the multilocus analysis). For PH and TGW,
421 only three and six regions, respectively, were detected in single trials (with a maximum
422 coincidence of five trials), much less than those identified by the meta-analysis. For grain
423 yield, there were more regions detected in single trials, altogether 125 MTAs in 20

424 regions, compared to the 11 QTLs found in the meta-analysis. However, with a threshold
425 of five, the number of MTAs dropped to 48 (in two QTL regions), zero, six (in one QTL),
426 and 34 (in nine QTL regions), for HD, TGW, PH, and GY, respectively.

427 Overall, the meta-analysis increased the power of QTL detection; the confidence on the
428 main-effect QTLs, particularly those in the multilocus analyses, is high. The more trials
429 involved, the greater power of detection achieved. We were able to detect QTL effects
430 as low as just above 1% of the traits' variances. The stringent permutation test which
431 was used protects against false positives. A strict LD control to determine the confidence
432 intervals, and the use of multilocus models, restricted the number of QTLs detected even
433 further, but we still found a high number of QTLs. Besides the increased power of the
434 meta-analysis, breaking down the analysis by the main G x E component detected for
435 HD and PH revealed QTLs and candidate genes specific for certain conditions, such as
436 sowing date (autumn/spring) or latitude. The unique behaviour of cultivars Mona and
437 Saana is likely caused by their carrying the same mutant allele in a major flowering time
438 gene, *HvELF3* (Faure et al., 2012, Göransson et al., 2021). This causes them to bypass the
439 photoperiod sensitivity mechanism, leading to early flowering irrespective of the
440 daylength. This fact makes them relatively early in Southern environments, in which
441 most of the growing period occurs under short photoperiod.

442 The QTL regions found in this study were compared with those of recent studies
443 involving large populations and SNP genotyping, therefore allowing direct comparison.
444 First, the co-localisation of plant height QTLs with those reported by Tondelli et al. (2013)
445 was rather high. This is not surprising, as our genotype set is a subsample of theirs (they
446 used a 216 spring two-rowed panel), and some trials were also shared (those from 2009
447 and 2010). We found 29 PH QTLs, compared with 17 found in Tondelli et al. (2013). Out
448 of those 17 PH QTLs, 11 were inside the confidence intervals of our QTLs (PH1, PH2, PH4,
449 PH6, PH11, PH13, PH14, or very close to them PH15, PH20, PH25, PH29). Plant height
450 QTL derived from part of our trials (2016 and 2017) were reported by Bretani et al.
451 (2022). They studied a larger diversity panel, comprising 165 two-rowed (including our
452 entire panel), and 96 six-rowed barleys. They found 48 PH QTL, 26 of them either in the
453 two-rowed or in the whole panel. Twelve of those 26 were inside the confidence
454 intervals of nine of our QTLs (PH2, PH3, PH4, PH5, PH8, PH13, PH14, PH20, PH28). None
455 of our QTLs coincided with their 22 six-rowed specific QTLs.

456 The same association panel as Tondelli et al. (2013) was studied by Xu et al. (2018). In
457 this case, only two QTLs, one for grain yield (GY6) and one for thousand grain weight

458 (TGW18), are shared with our results. This low number of matches could be explained
459 by different methodologies for QTL detection. Multilocation QTL analysis was run using
460 Genstat software, which allows finding QTL in interactions with the environment. As
461 mentioned above, the meta-analysis focuses on QTLs with low interaction. Out of the
462 23 QTLs detected for GY and TGW in the work by Xu et al. (2018), only eight were
463 detected as the main factor QTL (i.e., not interacting with the environment) and one of
464 them coincided with a TGW found in our study.

465 Bustos-Korts et al. (2019) studied a highly diverse panel of 371 genotypes including
466 landraces and cultivars, two- and six-rowed, winter and spring barley. They scored plant
467 height, thousand grain weight, and flowering time (Z55) in common with our study. Two
468 QTLs are shared for flowering time (HD12 and HD13), one of them in the region of
469 *HvVRN2*. For plant height, two QTLs have matching confidence intervals (PH8 and PH14);
470 *sdw1* is within one of them. For TGW, there is no QTL in common, although they found
471 a QTL for this trait close to the *Vrs1* gene, which is the same location as our QTL GY2.

472 Recently, a large association panel ($n = 363$) of European two-rowed spring barley was
473 analysed for flowering time, plant height, and thousand grain weight (Bernd et al.,
474 2024). One QTL for flowering time on chromosome 6H had overlapping confidence
475 intervals with HD17. Meanwhile, one MTA for plant height is within PH14, where *sdw1*
476 is located, while another one on chromosome 7H is close to PH25, where their LD block
477 should overlap. For thousand grain weight, one of their four QTLs has also been
478 identified in this study (TGW9, chromosome 3H).

479 We found evidence of surprisingly highly colocalizing QTLs in a recent study addressing
480 two- and six-rowed spring barley germplasm, which was less related to our panel than
481 that of other previous studies. Two articles published using a diverse multi-parent barley
482 population found new QTLs with minor to moderate phenotypic effects (Shrestha et al.,
483 2022; Cosenza et al., 2024). Several of our HD QTLs co-located with those found in
484 Cosenza et al. (2024): HD3, HD4, HD10, HD15, and HD17 had overlapping confidence
485 intervals with QTLs found in the multi-parent population analysis; whereas QTLs
486 overlapping with HD5, HD13 and HD22 were detected in single populations. For plant
487 height, 14 of the 29 QTLs (Table 3) co-located with QTLs for the same trait in the multi-
488 parent population. Most of them were detected in single populations, but three (PH15,
489 PH22, PH24) were detected in the whole population. Regarding thousand grain weight,
490 out of the 27 QTLs found in our study, 10 coincided with TGW QTLs in the multi-parent
491 population (Shrestha et al., 2022).

492 The population studied by Shrestha et al. (2022) and Cosenza et al. (2024) is composed
493 of two-row and six-row subpopulations and, thus, probably represents a larger genetic
494 diversity space than our panel. Moreover, the multi-parent population they used is more
495 amenable to the detection of small effect QTLs. In any case, the multiple shared
496 locations for QTLs in our study and theirs is likely a result of the higher power of
497 detection achieved with either approach, thus providing further confidence in the
498 associations found in the present study. Therefore, the loci identified constitute a sound
499 set of QTLs, with a clear potential to contribute to barley breeding in Europe.

500 A recent study (Hong et al., 2024), using a large and diverse two-rowed barley panel,
501 found 38 MTAs for grain size, one in common with our TGW20 QTL. Finally, a meta-
502 analysis revising yield-related traits of 54 studies that were published since 2000 (Du et
503 al., 2024) found four QTLs co-locating with ours: TGW3, TGW17, TGW25 and GY2.

504 **Implications for breeding**

505 The major selection footprints that we found appeared to be associated with disease
506 resistance. We concentrated only on the most salient selective sweeps, although it is
507 evident that breeding affected allelic frequencies throughout the genome with the shifts
508 (large or small) paralleling always the time gradient (Fig. S10). The pericentromeric
509 region of 5H, and its possible relation to the introduction of leaf rust tolerance, was
510 thoroughly described in Wonneberger et al. (2023). Interestingly, the narrower, but
511 equally marked selection footprint of 5HL appears to be associated with two stem rust
512 resistance QTLs (Case et al., 2018). The selection footprint found in 4HL was not
513 associated with agronomic QTLs. The closest one was TGW13, 15 Mb away. However, a
514 QTL for net blotch tolerance, on the position of the selection footprints was found by
515 Daba et al. (2020).

516 The dynamics of the evolution of allele frequencies for the agronomic QTLs in the
517 timeframe of our study suggest an early selection of many plant height QTLs, followed
518 closely in time by selection for thousand grain weight. Not surprisingly, both traits
519 usually show high heritability. Effective selection for grain yield QTLs occurs later,
520 apparently facilitated once the variance for the other traits was reduced. Plant height is
521 easy to select, due to its high heritability, and shortness was preferred to minimize
522 lodging, particularly after the introduction of semi-dwarf alleles like *denso/sdw1*
523 (detected as PH14). Grain yield and thousand-grain weight were also important
524 breeding targets for production and quality, but their selection appeared stronger after
525 PH was improved. For instance, in the close QTL pairs PH1-TGW1, PH6-TGW4, PH15-

526 TGW10, PH4-GY1, and PH8-GY3 (Table S4), PH-favourable alleles were fixed, or almost
527 so, in the most modern class of cultivars, whereas the frequencies of favourable alleles
528 for the QTLs of the other trait were low (although already growing in some cases). This
529 was also the case for the region with QTL PH27-TGW26-GY9. In this region, modern
530 varieties have favourable alleles for GY and PH almost fixed, while the favourable TGW
531 allele frequency is still low. In other cases, favourable alleles for the two traits in a
532 particular region were found in intermediate frequencies throughout the breeding
533 history (PH10-TGW7, PH26-TGW25, PH13-TGW9, PH24-TGW21). Therefore, selection
534 for both favourable alleles is likely feasible although, in the last two cases, the genotypic
535 frequencies indicate a possible linkage in repulsion for the favourable alleles. In all other
536 cases, the favourable alleles had already been selected. These observations can be of
537 direct use for barley breeders.

538 GY7 showed the largest frequency shift, around 0.9, across time of all QTLs detected in
539 this study. It was very effectively selected throughout the second half of the 20th
540 Century. The QTLs PH19 and TGW15 lie close to GY7. These two QTLs share the flag
541 marker, although with opposite effects for agronomic fitness. One allele is associated
542 with low height and thin grains, and the other one to tall plants and large grains. The
543 antagonistic effect of a single gene on these two traits was already described for the
544 main semi-dwarfing gene in barley, *HvGA20ox2* (Thomas et al., 1991). In this case,
545 breeding selected short plants preferentially over large grains, although grain weight
546 may have been compensated by selection at other loci. A possible explanation of the
547 historic trends observed is that, once the PH19/TGW15 QTL was almost fixed for short
548 plants, selection for grain yield at this region was facilitated. Indeed, favourable alleles
549 for low TGW and plant height appear together in 142 cultivars, whereas the only nine
550 cultivars with the “elevated height” allele also present the “high TGW” allele.

551 The near fixation of favourable alleles for traits which suffered strong selection pressure
552 on neighbouring QTLs may have helped the selection at GY7. A similar situation may
553 have occurred at 5HL, where the near fixation of the favourable (low height) allele at
554 PH22, may have strengthened selection near TGW18, whose favourable allele suffered
555 strong selection over time. The proximity of some QTLs and their fates throughout
556 breeding suggests possible targets for future breeding. For example, in the distal region
557 of 3HL, PH15 shows a decreasing frequency of “high” alleles, indicating selection
558 pressure; however, the favourable allele of the neighbouring QTL, TGW10, remains at a
559 low frequency. This suggests the presence of linked favourable alleles in repulsion, a

560 situation that could be addressed by breeding. A similar phenomenon occurs at the
561 beginning of 2H, with QTL PH6 and TGW4.

562 **Candidate genes**

563 Some candidate loci corresponded to the already-known functions of characterised
564 genes, while loci either provided new information about the effects of known genes or
565 revealed genes with unknown roles in barley, but with suggested ones based on
566 orthologues in rice (Table 5). For example, the candidate gene for HD17 is a homologue
567 of *Arabidopsis thaliana AtNUP160*, associated with flowering time (Li et al., 2020). It
568 anchors HOS1 to the ubiquitinated CONSTANS protein, which has not been reported in
569 barley so far. Further evidence for the possible involvement of this gene in flowering
570 comes from its preferential expression in barley apical meristems, inflorescences, and
571 microspores (Li et al., 2023).

572 Looking at the confidence intervals of HD QTLs, several known flowering-related genes
573 were located within them. Among these 22 QTLs, the confidence regions included
574 *HvCO9* (Cockram et al., 2012), *HvFT3* (Faure et al., 2007, Kikuchi et al., 2009), *HvHAP3*
575 (Campoli et al., 2013), and *HvVRN2* (Karsai et al., 2005), respectively in HD3, HD4, HD6,
576 and HD13. However, *HvFT3* is not a good candidate, since all 151 cultivars have the same
577 (presence) allele at this gene. Similarly, *HvVRN2* is not a likely candidate, as the allelic
578 segregation for this gene does not coincide with that of the QTL (Table S1). On the
579 contrary, three more QTLs were located near flowering-related genes that are good
580 candidates: HD13 was only 3 Mb apart from *HvFT5* (Faure et al., 2007, Kikuchi et al.,
581 2009), HD21 was 5.5 Mb away from *HvMADS26* (Pankin et al., 2018, Hill et al., 2019),
582 and HD16 was 383 kb away of *HvFRI* (Campoli et al., 2013).

583 The candidate gene for the plant height QTL PH24 corresponds to the orthologous one
584 in rice, *LAI1/LAZY1*. This gene regulates the expression of auxin transporters to control
585 tiller angle and shoot gravitropism (Li et al., 2007; Zhu et al., 2020). Interestingly, a
586 candidate gene for the thousand-grain weight QTL TGW18 is the orthologue of rice
587 *OsBRXL4*, which is a regulator of the nuclear localization gene of rice *LAI1/LAZY1* (Li et
588 al., 2019). Although neither rice gene has been studied for grain weight, they are highly
589 related to plant architecture. There is a possible candidate locus affecting two QTLs on
590 7HL, PH29 and GY11. The candidate is a cluster of four orthologues of the rice gene
591 *OsMPH1/OsMYB45*, located exactly in the overlapping interval of the two QTLs. This rice
592 gene affects plant height and grain yield (Zhang et al., 2017), which is consistent with
593 our observations. The favourable alleles at these two QTL were present at high

594 frequencies, and both increased over time until fixation, indicating joint selection in this
595 region.

596 The *HvHOX1* (*Vrs1*) gene is a candidate for QTL GY2. The haplotype *Vrs1.t*, commonly
597 known as *deficiens* (Sakuma et al., 2017) could underlie the favourable allele, providing
598 a yield advantage of 0.28 t ha⁻¹ across all trials. Selection at this QTL apparently started
599 in the 1980-90s and was subject to strong selection pressure. This allele conferred larger
600 grains, although this did not result in a yield advantage in the study by Sakuma et al
601 (2017). Those authors hypothesized that *deficiens* induces larger grains by the
602 suppression of organs (lateral florets), not specifically involved in sink/source
603 relationships. In our study, however, this QTL did not show a clear signal for TGW, but
604 the GY response was very consistent across environments. To the best of our knowledge,
605 this is the first time that a yield advantage has been reported for this gene under field
606 conditions.

607 In summary, our results indicate when and where breeding removed allelic diversity,
608 which traits were more accessible to breeders, where there were effects on nearby
609 genes, and how. When combined with candidate gene identification, our approach
610 allows the biological function of gene under relevant field conditions to be examined.
611 This information, in sum, provides a road map to help breeders fine tuning their targets
612 for the future.

613 **Supplementary data**

614 Supplementary Table S1. List of 164 genotypes, with country and release year. Allelic
615 data for flowering-related genes and *Vrs1*.

616 Supplementary Table S2. Information of the field trial network and best spatial
617 correction models.

618 Supplementary Table S3. Summary of MTAs of single-trial GWAS.

619 Supplementary Table S4. Co-localisation of meta-QTLs between traits.

620 Supplementary Table S5. Summary of meta-QTLs enrichment with exome capture
621 markers.

622 Supplementary Table S6. BLUEs of the four phenotypic traits evaluated.

623 Supplementary Table S7. Genotypic data of 151 two-rowed spring barleys

624 Supplementary Figure S1. PCA of the 164 genotypes, showing which were selected for
625 further analyses.

626 Supplementary Figure S2. Correlation between trials for each trait.

627 Supplementary Figure S3. Kinship matrix of the selected 151 genotypes.

628 Supplementary Figure S4. Boxplots for all phenotypes and trials, divided by groups of
629 release year.

630 Supplementary Figure S5. Linear relationships between grain yield with plant height and
631 thousand-grain weight.

632 Supplementary Figure S6. Biplots of AMMI analyses for plant height, thousand-grain
633 weight and grain yield.

634 Supplementary Figure S7. Differences in heading time between the mean of each trial
635 with genotypes Saana and Mona.

636 Supplementary Figure S8. Manhattan plots of the meta-GWAS, for flowering time, plant
637 height and thousand-grain weight.

638 Supplementary Figure S9. Changes in allele frequencies over time of flowering time and
639 thousand-grain weight meta-QTLs.

640 Supplementary Figure S10. Genome-wide fingerprints of selection.

641 Supplementary Figure S11. Photo of the spikes from the 14 genotypes with the
642 favourable allele of QTL GY2, linked to *Vrs1*.

643 **Acknowledgements**

644 The authors are grateful to all technicians who participated in both European projects.

645 **Author contributions**

646 Funding was acquired by AMC, LC, BK, AG, RW, AJF, KP, AHS, LR, EI. The study was
647 conceptualized by AMC, AT, LC, BK, JR, RW, WT, KP, AHS, AV, LR and EI. Resources were
648 provided by AMC, LC, BK, AG, RW, KP, AHS, LR. Field experiments and data collection
649 were carried out by AMC, AT, SD, RS, CC, JR, LR, WT, FS, KP, AHS, MJ, FLS, MP, AV, SS and
650 EI. Methodology was designed by FMT, AT, LR, WT, SS, EI. Data curation was carried out
651 by FMT, AT, WT, AJF, SS and EI. Analyses were performed by FMT, AT, WT and EI. The
652 study was managed by AMC, LC, BK, RW, WT, KP, AHS, FLS, AV, LR. Analyses and plotting
653 code were written by FMT, WT and EI. The research was supervised AMC, AT, LC, BK,

654 RW, WT, KP, AHS, FLS, AV and LR. Plots were created by FMT, AMC and EI. Original draft
655 was prepared by FMT, AMC, AT and EI. All authors revised the final manuscript.

656 **Conflict of interest**

657 The authors declare no conflict of interest.

658 **Funding**

659 This work was supported by the ERA-PG-funded project Exbardiv (Genomics-Assisted
660 Analysis and Exploitation of Barley Diversity; <http://www.erapg.org>), the FACCE ERA-
661 NET Plus project ClimBar 618105 (An integrated approach to evaluate and utilise genetic
662 diversity for breeding climate-resilient barley), the SUSCROP ERA-NET project BARISTA
663 PCI2019-103758 (Advanced tools for breeding BARley and Intensive and SusTainable
664 Agriculture under climate change scenarios), and by the Government of Aragón grants
665 A08_20R and A08_23R. FMT PhD scholarship was funded by the Government of Aragón,
666 2019-2023. FMT one-month traineeship at James Hutton Institute, under the
667 supervision of LR, was funded by CSIC mobility project LINKB20052 (Barley adaptation
668 under climate change. Timing and efficiency of flowering).

669 **Data availability**

670 The phenotypic and genotypic data that support the findings of this study are provided
671 as supplementary Tables S6 and S7, respectively.

REFERENCES

Andriotis VM, Saalbach G, Waugh R, Field RA, Smith AM (2016) The maltase involved in starch metabolism in barley endosperm is encoded by a single gene. PLoS One 11:e0151642. <https://doi.org/10.1371/journal.pone.0151642>

Bayer MM, Rapazote-Flores P, Ganal M, Hedley PE, Macaulay M, Plieske J, Ramsay L, Russell J, Shaw PD, Thomas W, Waugh R (2017) Development and Evaluation of a Barley 50k iSelect SNP Array. Front Plant Sci 8:1792. <https://doi.org/10.3389/fpls.2017.01792>

Bernad V, Al-Tamimi N, Langan P, Gillespie G, Dempsey T, Henchy J, Harty M, Ramsay L, Houston K, Macaulay M, Shaw PD, Raubach S, Mcdonnel KP, Russell J, Waugh R,

Khodaeiaminjan M, Negrão S (2024) Unlocking the genetic diversity and population structure of the newly introduced two-row spring European Heritage Barley collection (ExHIBiT). *Front Plant Sci* 15:1268847. <https://doi.org/10.3389/fpls.2024.1268847>

Bresghello F, Sorrells ME (2006) Association mapping of kernel size and milling quality in wheat (*Triticum aestivum* L.) cultivars. *Genetics* 172:1165-1177. <https://doi.org/10.1534/genetics.105.044586>

Bretani G., Shaaf S, Tondelli A, Cattivelli L, Delbono S, Waugh R, Thomas W, Russell J, Bull H, Igartua E, Casas AM, Gracia P, Rossi R, Schulman AH, Rossini L (2022) Multi-environment genome-wide association mapping of culm morphology traits in barley. *Front Plant Sci* 13:926277. <https://doi.org/10.3389/fpls.2022.926277>

Browning BL, Zhou Y, Browning SR (2018) A one-penny imputed genome from next-generation reference panels. *Am J Hum Genet* 103:338-348. <https://doi.org/10.1016/j.ajhg.2018.07.015>

Bucher CA, Azevedo Santos L, de Matos Nogueira E, Passos Rangel R, Regina de Souza S, Silvestre Fernandes M (2014) The transcription of nitrate transporters in upland rice varieties with contrasting nitrate-uptake kinetics. *J Plant Nutr Soil Sci*, 177: 395-403. <https://doi.org/10.1002/jpln.201300086>

Bull H, Casao MC, Zwirek M, Flavell AJ, Thomas WTB, Guo W, Zhang R, Rapazote-Flores P, Kyriakidis S, Russell J, Druka A, McKim SM, Waugh R (2017) Barley SIX-ROWED SPIKE3 encodes a putative Jumonji C-type H3K9me2/me3 demethylase that represses lateral spikelet fertility. *Nat Comm* 8:936. <https://doi.org/10.1038/s41467-017-00940-7>

Bustos-Korts D, Dawson IK, Russell J, Tondelli A, Guerra D, Ferrandi C, Strozzi F, Nicolazzi EL, Molnar-Lang M, Ozkan H, Megyeri M, Miko P, Çakır E, Yaklışır E, Trabanco N, Delbono S, Kyriakidis S, Booth A, Cammarano D, Mascher B, Werner P, Cattivelli L, Rossini L, Stein N, Kilian B, Waugh R, van Eeuwijk FA (2019) Exome sequences and multi-environment field trials elucidate the genetic basis of adaptation in barley. *Plant J* 99:1172-1191. <https://doi.org/10.1111/tpj.14414>

Campoli C, Pankin A, Drosse B, Casao CM, Davis SJ, von Korff M (2013) *HvLUX1* is a candidate gene underlying the *early maturity 10* locus in barley: phylogeny, diversity, and interactions with the circadian clock and photoperiodic pathways. *New Phytol* 199:1045–1059. <https://doi.org/10.1111/nph.12346>

Case AJ, Bhavani S, Macharia G, Steffenson BJ (2018) Genome-wide association study of stem rust resistance in a world collection of cultivated barley. *Theor Appl Genet* 131:107–126. <https://doi.org/10.1007/s00122-017-2989-y>

Chen YY, Schreiber M, Bayer MM, Dawson IK, Hedley PE, Lei L, Akhunova A, Liu C, Smith KP, Fay JC, Muehlbauer GJ, Steffenson BJ, Morrell PL, Waugh R, Russell JR (2022) The evolutionary patterns of barley pericentromeric chromosome regions, as shaped by linkage disequilibrium and domestication. *Plant J* 111:1580-1594. <https://doi.org/10.1111/tpj.15908>

Cockram J, Thiel T, Steuernagel B, Stein N, Taudien S, Bailey PC, O'Sullivan DM (2012) Genome dynamics explain the evolution of flowering time CCT domain gene families in the Poaceae. *PLoS ONE* 7:e45307. <https://doi.org/10.1371/journal.pone.0045307>

Cosenza F, Shreshta A, van Inghelandt D, Casale FA, Wu PY, Weisweiler M, Li J, Wespel F, Stich B (2024). Genetic mapping reveals new loci and alleles for flowering time and plant height using the double round-robin population of barley. *J Exp Bot* 75:2385-2402. <https://doi.org/10.1093/jxb/erae010>

Daba SD, Horsley R, Brueggeman R, Chao S, Mohammadi M (2019). Genome-wide association studies and candidate gene identification for leaf scald and net blotch in barley (*Hordeum vulgare* L.). *Plant Dis.* 103:880-889. <https://doi.org/10.1094/PDIS-07-18-1190-RE>

Dawson IK, Russel J, Powell W, Steffenson B, Thomas WTB, Waugh R (2015) Barley: a translational model for adaptation to climate change. *New Phytol* 206:913-931. <https://doi.org/10.1111/nph.13266>

Delignette-Muller ML, Dutang C (2015) *fitdistrplus*: An R package for fitting distributions. *J Stat Soft* 64:1-34. <https://doi.org/10.18637/jss.v064.i04>

Du B, Wu J, Wang Q, Sun C, Sun G, Zhou J, Zhang L, Xiong Q, Ren X, Lu B (2024) Genome-wide screening of meta-QTL and candidate genes controlling yield and yield-related traits in barley (*Hordeum vulgare* L.). *PLOS One* 19:e0303751. <https://doi.org/10.1371/journal.pone.0303751>

Dziurdziak J, Podyma W, Bujak H, Boczkowska M (2022) Tracking changes in the spring barley gene pool in Poland during 120 years of breeding. *Int J Mol Sci* 23:4553. <https://doi.org/10.3390/ijms23094553>

Faure S, Higgins J, Turner A, Laurie DA (2007) The *FLOWERING LOCUS T*-like gene family in barley (*Hordeum vulgare*). Genetics 176:599–609. <https://doi.org/10.1534/genetics.106.069500>

Faure S, Turner AS, Gruszka D, Christodoulou V, Davis SJ, von Korff M, Laurie DA (2012) Mutation at the circadian clock gene *EARLY MATURITY 8* adapts domesticated barley (*Hordeum vulgare*) to short growing seasons. Proc Natl Acad Sci USA 109:8328-8333. <https://doi.org/10.1073/pnas.1120496109>

Fox J, Weisberg S (2019) An R companion to applied regression, third edition. Sage, Thousand Oaks CA. <https://socialsciences.mcmaster.ca/jfox/Books/Companion/>.

Göransson M, Sigurdardottir TH, Lillemo M, Bengtsson T, Hallsson JH (2021) The winter-type allele of HvCEN is associated with earliness without severe yield penalty in icelandic spring barley (*Hordeum vulgare* L.). Front Plant Sci 12:720238. <https://doi.org/10.3389/fpls.2021.720238>

Hill CB, Angessa TT, McFawn LA, Wong D, Tibbets J, Zhang XQ, Forrest K, Moody D, Telfer P, Westcott S, Diepeveen D, Xu Y, Tan C, Hayden M, Li C (2019) Hybridisation-based target enrichment of phenology genes to dissect the genetic basis of yield and adaptation in barley. Plant Biotech J 17:932–944. <https://doi.org/10.1111/pbi.13029>

Hong Y, Zhang M, Zhu J, Zhang Y, Lv C, Guo B, Wang F, Xu R (2024) Genome-wide association studies reveal novel loci for grain size in two-rowed barley (*Hordeum vulgare* L.). Theor Appl Genet 137:58. <https://doi.org/10.1007/s00122-024-04562-8>

Huang S, Zhang A, Jin JB, Zhao B, Wang TJ, Wu Y, Wang S, Liu Y, Wang J, Guo P, Ahmad R, Liu B, Xu ZY (2019) Arabidopsis histone H3K4 demethylase JMJ 17 functions in dehydration stress response. New Phytol 223:1372-1387. <https://doi.org/10.1111/nph.15874>

Huang F, Jiang Y, Chen T, Li H, Fu M, Wang Y, Xu Y, Li Y, Zhou Z, Jia L, Ouyang W, Yao W (2022) New data and new features of the FunRiceGenes (functionally characterized rice genes) database: 2021 update. Rice, 15:23. <https://doi.org/10.1186/s12284-022-00569-1>

Igartua E, Cantalapiedra CP, Casas AM (2019) Genome-wide association studies (GWAS) in barley. In Advances in breeding techniques for cereal crops (pp. 503-536). Burleigh Dodds Science Publishing.

Jayakodi M, Padmarasu S, Haberer G, Bonthala VS, Gundlach H, Monat C, Lux T, Kamal N, Lang D, Himmelbach A, Ens J, Zhang XQ, Angessa TT, Zhou G, Tan C, Hill C, Wang P, Schreiber M, Boston LB, Plott C, Jenkins J, Guo Y, Fiebig A, Budak H, Xu D, Zhang J, Wang C, Grimwood J, Schmutz J, Guo G, Zhang G, Mochida K, Hirayama T, Sato K, Chalmers KJ, Langridge P, Waugh R, Pozniak CJ, Scholz U, Mayer KFX, Spannagl M, Li C, Mascher M, Stein N (2020) The barley pan-genome reveals the hidden legacy of mutation breeding. *Nature* 588:284-289. <https://doi.org/10.1038/s41586-020-2947-8>

Karsai I, Szűcs P, Mészáros K, Filichkina T, Hayes PM, Skinner JS, Láng L, Bedő Z (2005) The *Vrn-H2* locus is a major determinant of flowering time in a facultative x winter growth habit barley (*Hordeum vulgare* L.) mapping population. *Theor Appl Genet* 110:1458–1466. <https://doi.org/10.1007/s00122-005-1979-7>

Kikuchi R, Kawahigashi H, Ando T, Tonooka T, Handa H (2009) Molecular and functional characterization of PEBP genes in barley reveal the diversification of their roles in flowering. *Plant Physiol* 149:1341–1353. <https://doi.org/10.1104/pp.108.132134>

Kolodinska Brantestam A, Von Bothmer R, Dayteg C, Rashal I, Tuveson S, Weibull J (2004) Inter simple sequence repeat analysis of genetic diversity and relationships in cultivated barley of Nordic and Baltic origin. *Hereditas* 141:186-192. <https://doi.org/10.1111/j.1601-5223.2004.01867.x>

Komatsuda T, Pourkheirandish M, He C, Azhaguvvel P, Kanamori H, Perovic D, Stein N, Graner A, Wicker T, Tagiri A, Lundqvist U, Fujimura T, Matsuoka M, Matsumoto T, Yano M (2007) Six-rowed barley originated from a mutation in a homeodomain-leucine zipper I-class homeobox gene. *Proc Natl Acad Sci USA* 104:1424–1429. <https://doi.org/10.1073/pnas.060858010>

Li P, Wang Y, Qian Q, Fu Z, Wang M, Zeng D, Li B, Wang X, Li J (2007) LAZY1 controls rice shoot gravitropism through regulating polar auxin transport. *Cell Res* 17:402–410. <https://doi.org/10.1038/cr.2007.38>

Li C, Liu L, Teo ZWN, Shen L, Yu H (2020) Nucleoporin 160 regulates flowering through anchoring HOS1 for destabilizing CO in *Arabidopsis*. *Plant Comm* 1:100033. <https://doi.org/10.1016/j.xplc.2020.100033>

Li T, Li Y, Shangguan H, Bian J, Luo R, Tian Y, Li Z, Nie X, Cui L (2023) BarleyExpDB: an integrative gene expression database for barley. *BMC Plant Biol* 23:170. <https://doi.org/10.1186/s12870-023-04193-z>

Li Z, Liang Y, Yuan Y, Wang L, Meng X, Xiong G, Zhou J, Cai Y, Han N, Hua L, Liu G, Li J, Wang Y (2019) OxBRXL4 regulates shoot gravitropism and rice tiller angle through affecting LAZY1 nuclear localization. *Mol Plant* 12:1143-1156. <https://doi.org/10.1016/j.molp.2019.05.014>

Looseley ME, Ramsay L, Bull H, Swanston JS, Shaw PD, Macaulay M, Booth A, Russell JR, Waugh R, Thomas WTB (2020) Association mapping of malting quality traits in UK spring and winter barley cultivar collections. *Theor Appl Genet* 133:2567-2582. <https://doi.org/10.1007/s00122-020-03618-9>

Mangin B, Siberchicot A, Nicolas S, Doligez A, This P, Cierco-Ayrolles C (2012) Novel measures of linkage disequilibrium that correct the bias due to population structure and relatedness. *Heredity* 108:285–291. <https://doi.org/10.1038/hdy.2011.73>

Mascher M, Richmond TA, Gerhardt DJ, Himmelbach A, Clissold L, Sampath D, Ayling S, Steuernagel B, Pfeifer M, D'Ascenzo M, Akhunov ED, Hedley PE, Gonzales AM, Morrell PL, Kilian B, Blattner FR, Scholz U, Mayer KFX, Flavell AJ, Muehlbauer GJ, Waugh R, Juddeloh JA, Stein N (2013) Barley whole exome capture: a tool for genomic research in the genus *Hordeum* and beyond. *Plant J* 76:494–505. <https://doi.org/10.1111/tpj.12294>

Mascher M, Gundlach H, Himmelbach A, Beier S, Twardziok SO, Wicker T, Radchuk V, Dockter C, Hedley PE, Russell J, et al (2017) A chromosome conformation capture ordered sequence of the barley genome. *Nature* 544:427–433. <https://doi.org/10.1038/nature22043>

Mascher M, Wicker T, Jenkins J, Plott C, Lux T, Koh CS, Ens J, Gundlach H, Boston LB, Tulpová Z, Holden S, Hernández-Pinzón I, Scholz W, Mayer KFX, Spannagl M, Pozniak CJ, Sharpe AG, Šimková H, Moscou MJ, Grimwood J, Schmutz J, Stein N (2021) Long-read sequence assembly: a technical evaluation in barley. *Plant Cell* 33:1888-1906. <https://doi.org/10.1093/plcell/koab077>

Milne L, Bayer M, Rapazote-Flores P, Mayer CD, Waugh R, Simpson CG (2021) EORNA, a barley gene and transcript abundance database. *Sci Data* 8:90. <https://doi.org/10.1038/s41597-021-00872-4>

Muñoz-Amatriaín M, Hernandez J, Herb D, Baenziger PS, Bochard AM, Capettini F, Casas A, Cuesta-Marcos A, Einfeldt C, Fisk S, Genty A, Helgerson L, Herz M, Hu G, Igartua E, Karsai I, Nakamura T, Sato K, Smith K, Stockinger E, Thomas W, Hayes P (2020) Perspectives on low temperature tolerance and vernalization sensitivity in barley: prospects for facultative growth habit. *Front Plant Sci* 11:585927. <https://doi.org/10.3389/fpls.2020.585927>

Pankin A, Altmüller J, Becker C, von Korff M (2018) Targeted resequencing reveals genomic signatures of barley domestication. *New Phytol* 218:1247–1259. <https://doi.org/10.1111/nph.15077>

R Core Team (2024). R: A language and environment for statistical computing. R Foundation for Statistical Computing, Vienna, Austria. <https://www.R-project.org/>. Accessed 24 June 2024

Russell J, Mascher M, Dawson IK, Kyriakidis S, Calixto C, Freund F, Bayer M, Milne I, Marshall-Griffiths T, Heinen S, Hofstad A, Sharma R, Himmelbach A, Knauf M, van Zonneveld M, Brown JWS, Schmid K, Kilian B, Muehlbauer GJ, Stein N, Waugh R (2016) Exome sequencing of geographically diverse barley landraces and wild relatives gives insights into environmental adaptation. *Nat Genet* 48:1024-1030. <https://doi.org/10.1038/ng.3612>

Sakuma S, Lundqvist U, Kakei Y, Thirulogachandar V, Suzuki T, Hori K, Wu J, Tagiri A, Rutten T, Koppolu R, Shimada Y, Houston K, Thomas WTB, Waugh R, Schnurbusch T, Komatsuda T (2017). Extreme suppression of lateral floret development by a single amino acid change in the VRS1 transcription factor. *Plant Physiol* 175:1720-1731. <https://doi.org/10.1104/pp.17.01149>

Schmidt SB, Brown LK, Booth A, Wishart J, Hedley PE, Martin P, Husted S, George WS, Russell J. (2023) Heritage genetics for adaptation to marginal soils in barley. *Trends Plant Sci* 28:544:551. <https://doi.org/10.1016/j.tplants.2023.01.008>

Shrestha A, Cosenza F, van Inghelandt D, Wu P-Y, Li J, Casale FA, Weisweiler M, Stich B (2022) The double round-robin population unravels the genetic architecture of grain size in barley. *J Exp Bot* 73:7344–7361. <https://doi.org/10.1093/jxb/erac369>

Thomas WTB (2020) Advances in molecular breeding techniques for barley: genome-wide association studies (GWAS). In Achieving sustainable cultivation of barley (pp.183-202). Burleigh Dodds Science Publishing.

Thomas W, Powell W, Swanston J (1991) The effects of major genes on quantitatively varying characters in barley. 4. The GPer and denso loci and quality characters. *Heredity* 66:381–389. <https://doi.org/10.1038/hdy.1991.48>

Tondelli A, Xu X, Moragues M, Sharma R, Schnaithmann F, Ingvarsson C, Manninen O, Comadran J, Russell J, Waugh R, Schulman AH, Pillen K, Rasmussen SK, Kilian B, Cattivelli L, Thomas WTB, Flavell AJ (2013) Structural and temporal variation in genetic diversity of European spring two-row barley cultivars and association mapping of quantitative traits. *Plant Genome* 6:2. <https://doi.org/10.3835/plantgenome2013.03.0007>

van Esse GW, Walla A, Finke A, Koornneef M, Pecinka A, von Korff M (2017) Six-Rowed Spike3 (VRS3) is a Histone Demethylase that controls lateral spikelet development in barley. *Plant Physiol* 174:2397–2408. <https://doi.org/10.1104/pp.17.00108>

VSN International (2022). Genstat for Windows 22nd Edition. VSN International, Hemel Hempstead, UK. Web page: Genstat.co.uk

Wang J, Zhang Z (2021) GAPIT Version 3: boosting power and accuracy for genomic association and prediction. *Genom Proteom Bioinf* 19:629-640. <https://doi.org/10.1016/j.gpb.2021.08.005>

Willer CJ, Li Y, Abecasis GR (2010) METAL: fast and efficient meta-analysis of genomewide association scans. *Bioinformatics* 26:2190-2191. <https://doi.org/10.1093/bioinformatics/btq340>

Wonneberger R, Schreiber M, Haaning A, Muehlbauer GJ, Waugh R, Stein N (2023) Major chromosome 5H haplotype switch structures the European two-rowed spring barley germplasm of the past 190 years. *Theor Appl Genet* 136: 174. <https://doi.org/10.1007/s00122-023-04418-7>

Xu Y, Jia Q, Zhou G, Zhang XQ, Angessa T, Broughton S, Yan G, Zhang W, Li C (2017) Characterization of the *sdw1* semi-dwarf gene in barley. *BMC Plant Biol* 17:11. <https://doi.org/10.1186/s12870-016-0964-4>

Xu X, Sharma R, Tondelli A, Russell J, Comadran J, Schnaithmann F, Pillen K, Kilian B, Cattivelli L, Thomas WTB, Flavell AJ (2018) Genome-wide association analysis of grain yield-associated traits in a pan-European barley cultivar collection. *Plant Genome* 11:170073. <https://doi.org/10.3835/plantgenome2017.08.0073>

Yates AD, Allen J, Amode RM, et al (2022) Ensembl Genomes 2022: an expanding genome resource for non-vertebrates. *Nucleic Acids Res* 50(D1):D996–D1003. <https://doi.org/10.1093/nar/gkab1007>

Zadoks JC, Chang TT, Konzak CF (1974). A decimal code for the growth stages of cereals. *Weed research* 14: 415-421. <https://doi.org/10.1111/j.1365-3180.1974.tb01084.x>

Zhang Y, Yu C, Lin J, Liu J, Liu B, Wang J, Huang A, Li H, Zhao T (2017) *OsMPH1* regulates plant height and improves grain yield in rice. *PLoS ONE* 12:e0180825. <https://doi.org/10.1371/journal.pone.0180825>

Zheng X, Levine D, Shen J, Gogarten SM, Laurie C, Weir BS (2012) A high-performance computing toolset for relatedness and principal component analysis of SNP data. *Bioinformatics* 28:3326-3328. <https://doi.org/10.1093/bioinformatics/bts606>

Zhu M, Hu Y, Tong A, Yan B, Lv Y, Wang S, Ma W, Cui Z, Wang X (2020). LAZY1 controls tiller angle and shoot gravitropism by regulating the expression of auxin transporters and signaling factors in rice. *Plant Cell Physiol* 61:2111-2125. <https://doi.org/10.1093/pcp/pcaa131>

Table 1. Field trial network; locations and years. Phenotype means, standard deviation, and broad sense heritability.

Country	Trial code	Sowing date	Heading time (DAS)		Plant height (cm)		Grain yield (t/ha)		Thousand grain weight (g)	
			Mean	SD	Mean	SD	Mean	SD	Mean	SD
Morocco	MAR16	06/01/16	104.0	4.5	71.3	7.2	3.25	0.55	NA	NA
Spain	ESP16	11/11/15	163.7	6.6	63	8.8	2.98	0.67	33.2	3.3
Spain	ESP17	15/11/16	154.1	4.6	54.1	6.5	2.85	0.5	39.1	3
Italy	ITA16	05/11/15	167.8	4.0	86.4	6.9	7.98	1.13	38.4	5.2
Italy	ITA17	08/11/16	174.5	4.9	84.3	6.9	6.79	1.03	46.6	4.6
Italy	ITA09	17/02/09	96.3	2.9	65.3	6.1	4.55	0.74	43.6	3.1
Italy	ITA10	01/03/10	93.6	3.8	52.4	5.8	3.14	0.69	42.5	2.6
Germany	DE1-09	31/03/09	62.8	3.3	76.2	7.4	3.91	0.76	35.9	4.6
Germany	DE1-10	06/04/10	67.5	2.2	83.2	8.3	4.74	0.76	46.5	3.7
Germany	DE2-09	03/04/09	66.5	2.9	89.9	12.8	6.55	0.66	50.1	3.4
United Kingdom	GBR09	25/03/09	90.7	2.5	72.3	10.8	5.51	0.63	46.1	3.4
United Kingdom	GBR10	01/04/10	78.9	2.6	82	9.7	5.24	0.76	46.9	3.9
United Kingdom	GBR16	16/03/16	89.5	2.3	89.8	14.2	6.21	0.73	50.4	3.2
United Kingdom	GBR17	29/03/17	83.4	2.2	88.1	10.4	7.04	0.79	51.0	3.6
Finland	FIN16	11/05/16	53.3	3.4	49.4	6.3	2.94	0.6	35.8	3.1
Finland	FIN17	19/05/17	53.9	1.9	69.9	7.5	5.43	0.56	49.2	3.6
Heritability (h^2)			0.822		0.869		0.216		0.836	

Table 2. Multi-environment analysis of variance for BLUEs of four traits. Mean squares are presented (ms). As the replicate layer is not present, the variance ratio (vr) for genotype and environment is calculated with the G x E term in the denominator, becoming a stringent test, as this variance adds true G x E variance to the error variance. G x E variance is broken down in the first four components of an AMMI analysis for each trait, each tested for significance against the residual G x E variance left after removing the variance accounted for by each principal component (PC).

Source	df	Grain yield		Heading date		Plant height		Thousand grain weight	
		ms	vr	ms	vr	ms	vr	ms	vr
Genotype (G)	142	3.01	7.9**	117	27.9**	856	34.5**	124.9	22.3**
Environment (E)	15	397.3	1049.9**	249336	59620.4**	26706	1075.1**	5003.7	894.7**
G x E	2129	0.38		4		25		5.6	
IPCA 1	156	0.94	3.7**	23	12.1**	128	10.8**	17.3	5.3**
IPCA 2	154	0.68	2.7**	6	3.0**	47	3.9**	10.5	3.2**
IPCA 3	152	0.62	2.4**	5	2.9**	28	2.4**	8.1	2.5**
IPCA 4	150	0.45	1.8**	4	2.2**	23	1.9**	7.6	2.3**
Residuals	1517	0.26		2		12		3.2	

Table 3. Codes, positions, and significance of QTLs detected in the meta-analyses for the four traits studied. The last two columns correspond to the meta-analyses carried out splitting the trials in two subsets, according to the main genotype-by-environment trends found for HD and PH.

Trait	QTL	Flag marker	CHR	Position (bp)	MAF (%)	-log10(P)	CI Left	CI Right	Frequency shift	AUTUMN-log(P)	SPRING-log(P)
HD	HD1	JHI-9615	1H	9334749	7.95	21.59	8657247	10012251	-0.0198	4.65	18.09
HD	HD2	JHI-22609	1H	288026140	23.18	15.78	227188624	348863656	0.0278	5.28	11.20
HD	HD3	JHI-30295	1H	393403435	8.61	20.22	370210929	416595941	-0.0754	12.66	9.74
HD	HD4	JHI-40964	1H	473573354	14.57	22.66	463423350	483723358	0.0833	8.67	14.84
HD	HD5	JHI-79301	2H	48535423	21.85	18.87	43707921	53362925	0.3175	1.69	20.10
HD	HD6	JHI-84334	2H	80227961	8.61	13.12	54440457	106015465	0.1667	1.71	20.41
HD	HD7	JHI-139077	2H	650766414	6.62	32.33	648843896	652688932	-0.0556	11.91	21.32
HD	HD8	JHI-160692	3H	21859520	28.48	17.77	20147016	23572024	0.3334	1.06	20.39
HD	HD9	JHI-195020	3H	520711672	7.28	16.69	516881670	524541674	-0.1111	6.36	11.08
HD	HD10	JHI-202588	3H	553851218	25.83	18.88	551156212	556546224	0.0437	6.50	13.12
HD	HD11	JHI-230339	4H	11284074	7.95	15.4	9756570	12811578	-0.0556	5.14	10.95
HD	HD12	JHI-258528	4H	553142475	21.85	16.45	550707467	555577483	-0.0873	3.52	13.95
HD	HD13	JHI-274290	4H	605288793	8.61	19.89	602946289	607631297	-0.0556	6.45	14.19
HD	HD14	JHI-281887	5H	10837439	17.22	16.11	9264937	12409941	-0.2977	5.62	11.19
HD	HD15	JHI-333135	5H	523882465	6.62	21.22	521534963	526229967	-0.0873	12.53	10.66
HD	HD16	JHI-363055	5H	580109624	5.96	17.67	578892122	581327125	-0.0397	5.52	12.89
HD	HD17	JHI-385161	6H	40578511	6.62	34.76	9871009	71286013	-0.1667	9.33	26.44
HD	HD18	JHI-449563	7H	15111871	34.44	28.74	12271867	17951874	0.1389	8.70	20.89
HD	HD19	JHI-465895	7H	61645217	29.14	19.9	55847715	67442719	-0.0952	9.40	11.63
HD	HD20	JHI-482284	7H	339274267	5.30	20.47	180054249	498494285	-0.1111	13.26	9.60
HD	HD21	JHI-487408	7H	445376601	5.30	18.13	411521597	479231605	-0.0556	13.14	7.80
HD	HD22	JHI-500129	7H	590186971	8.61	16.81	586726967	593646975	-0.1111	4.80	12.77

Trait	QTL	Flag marker	CHR	Position (bp)	MAF (%)	-log10(P)	CI Left	CI Right	Frequency shift		
HD	HDA1	JHI-36690	1H	439402226		9.45	431402226	447402226		19.67	0.73
									NORTH-log(P)	SOUTH-log(P)	
PH	PH1	JHI-10283	1H	10222515	26.49	14.32	8937513	11507517	0.2659	5.81	7.64
PH	PH2	JHI-26359	1H	341796547	21.85	22.67	307514031	376079063	0.3571	13.09	7.88
PH	PH3	JHI-31326	1H	399027554	39.74	22.42	377665052	420390056	0.6587	12.34	8.20
PH	PH4	JHI-50444	1H	497490361	5.30	15.61	496007859	498972863	0.1667	7.78	7.56
PH	PH5	JHI-71619	2H	21253094	28.48	27.93	19518088	22988100	0.3373	14.13	10.64
PH	PH6	SCRI_RS_207244	2H	43626804	25.83	21.73	39626802	47626806	0.0476	11.06	8.56
PH	PH7	JHI-102401	2H	545047467	21.85	11.96	531869961	558224973	0.2976	4.58	6.83
PH	PH8	JHI-127870	2H	630365638	48.34	27.41	627615632	633115644	0.7857	16.02	10.22
PH	PH9	JHI-149745	3H	2203527	5.96	14.65	0	5218531	0	7.90	7.67
PH	PH10	JHI-164742	3H	52796359	13.25	24.59	24821353	80771365	0.0834	13.56	10.08
PH	PH11	SCRI_RS_8664	3H	385814518	10.60	19.29	232594474	539034562	-0.0238	12.43	7.38
PH	PH12	JHI-192298	3H	501844817	5.96	14.24	492514815	511174819	0.0754	9.14	4.40
PH	PH13	JHI-197260	3H	529944715	38.41	42.18	521877213	538012217	0.4524	20.59	17.41
PH	PH14	JHI-204986	3H	562585430	29.80	32.94	560745422	564425438	0.5952	13.25	16.58
PH	PH15	JHI-224935	3H	617619009	39.07	17.53	615594005	619644013	0.504	4.44	8.91
PH	PH16	JHI-233087	4H	28157377	17.22	20.19	23844871	32469883	0.3889	10.20	7.95
PH	PH17	JHI-259677	4H	561914675	27.15	13.69	560192173	563637177	0.1032	5.62	6.22
PH	PH18	SCRI_RS_25685	4H	579246000	10.60	25.94	575945996	582546004	0.1865	15.18	9.10
PH	PH19	JHI-281008	5H	9003891	5.96	17.44	8228889	9778893	0.0556	9.71	7.81
PH	PH20	JHI-325973	5H	510459720	23.18	22.05	505807218	515112222	0.4643	14.83	8.29
PH	PH21	JHI-344172	5H	545071584	49.67	14.41	542706564	547436604	0.6548	6.04	7.00
PH	PH22	JHI-363188	5H	580264475	7.95	17.86	579106973	581421977	-0.0873	6.24	9.81
PH	PH23	JHI-376336	6H	16037775	11.26	20.81	15397771	16677779	0.0437	12.08	7.24
PH	PH24	JHI-432554	6H	558950326	37.09	28.17	553850324	564050327	-0.0595	13.31	13.36
PH	PH25	JHI-456995	7H	31631859	29.80	23.12	26229343	37034375	0.246	11.63	8.72

Trait	QTL	Flag marker	CHR	Position (bp)	MAF (%)	-log10(P)	CI Left	CI Right	Frequency shift		
PH	PH26	SCRI_RS_235584	7H	435303585	36.42	17.59	404683581	465923589	-0.0675	7.33	9.58
										NORTH-log(P)	SOUTH-log(P)
PH	PH27	JHI-488571	7H	484010786	5.30	12.51	470178282	497843290	0.0556	6.92	4.42
PH	PH28	JHI-493193	7H	567606818	39.07	22.06	562011816	573201820	0.2778	14.52	5.61
PH	PH29	JHI-501203	7H	593432421	5.30	25.17	590122417	596742424	0.2223	12.88	10.89
TGW	TGW1	JHI-8460	1H	8528373	6.62	13.39	7915871	9140874	-0.0714		
TGW	TGW2	JHI-30897	1H	395769146	9.93	10.34	373764140	417774151	-0.1508		
TGW	TGW3	JHI-37341	1H	445816857	32.45	14.04	433116855	458516859	-0.0873		
TGW	TGW4	JHI-78063	2H	43791847	6.62	13.59	39781845	47801846	-0.1587		
TGW	TGW5	JHI-143015	2H	657064597	7.95	22.00	653724591.5	660404602	-0.131		
TGW	TGW6	JHI-148635	3H	317035	13.25	13.01	0	1259307	-0.1865		
TGW	TGW7	JHI-164082	3H	36220523	15.89	11.36	31745517	40695529	-0.2302		
TGW	TGW8	JHI-186657	3H	467575649	45.03	11.72	452938141	482213156	0.0198		
TGW	TGW9	JHI-199513	3H	539898192	6.62	20.74	531870684	547925700	0.0198		
TGW	TGW10	JHI-224889	3H	616943116	5.30	12.63	614920612	618965619	0.1111		
TGW	TGW11	JHI-230271	4H	11066831	17.22	16.95	9536827	12596834	-0.0238		
TGW	TGW12	JHI-236625	4H	50716395	10.60	14.12	33296389	68136400	-0.0953		
TGW	TGW13	SCRI_RS_159331	4H	546549711	9.93	13.14	543149703	549949719	-0.0873		
TGW	TGW14	JHI-266331	4H	588890830	27.15	16.52	585968326	591813334	-0.5357		
TGW	TGW15	JHI-281008	5H	9003828	5.96	13.76	8228826	9778830	0.0556		
TGW	TGW16	JHI-308899	5H	441356776	27.81	18.68	434834272	447879279	0.0635		
TGW	TGW17	SCRI_RS_165578	5H	533639048	13.91	20.99	531739042	535539053	-0.1032		
TGW	TGW18	JHI-364661	5H	582365354	41.72	22.95	581067852	583662855	-0.4683		
TGW	TGW19	JHI-381643	6H	31250013	11.92	13.95	27115011	35385014	-0.0119		
TGW	TGW20	JHI-402516	6H	388187724	49.67	13.84	359287700	417087747	-0.3095		
TGW	TGW21	JHI-433405	6H	560487100	17.88	18.04	546287100	574687100	-0.0675		

Trait	QTL	Flag marker	CHR	Position (bp)	MAF (%)	-log10(P)	CI Left	CI Right	Frequency shift
TGW	TGW22	JHI-452562	7H	20790898	11.26	13.32	18458394	23123401	0.1111
TGW	TGW23	JHI-478583	7H	254515002	5.96	13.60	245715002	263315002	0.0198
TGW	TGW24	JHI-483539	7H	386803631	44.37	10.71	212081113	561526149	0.1071
TGW	TGW25	JHI-486280	7H	441942697	41.72	18.48	382762693	501122701	-0.004
TGW	TGW26	JHI-488064	7H	479905076	41.06	14.31	465226728	494583424	-0.2222
TGW	TGW27	JHI-519440	7H	630314109	6.62	15.08	626879105	633749113	-0.0159
GY	GY1	JHI-50447	1H	497490053	11.26	11.30	495987551	498992555	-0.3571
GY	GY2	JHI-107800	2H	571877011	9.93	15.69	558557009	585197013	-0.4286
GY	GY3	JHI-126025	2H	626362758	7.28	12.11	624117756	628607760	-0.3214
GY	GY4	JHI-144055	2H	657925477	8.61	11.33	651895471	663955483	-0.1667
GY	GY5	JHI-153479	3H	7136438	21.85	11.19	4503934	9768942	-0.1389
GY	GY6	JHI-226878	4H	2316928	15.23	9.74	974426	3659430	-0.4087
GY	GY7	JHI-279907	5H	6585842	31.79	9.86	5450840	7720844	-0.9286
GY	GY8	JHI-441782	7H	6202146	12.58	11.76	4697144	7707146	-0.2778
GY	GY9	JHI-489124	7H	496874345	5.30	11.39	483214341	510534349	-0.0556
GY	GY10	JHI-492462	7H	559843244	11.93	21.14	293446961	632540561	-0.0556
GY	GY11	JHI-504313	7H	598982630	8.61	18.35	595532628	602432632	-0.2222

Table 4. Summary of QTLs kept in the multivariate multilocus analysis for the four studied traits.

Trait	Chr	QTL	Best model	Partial Eta2	Percentage of explained variance
HD	1H	HD1	*	0.20	1.39
HD	2H	HD5	***	0.37	2.89
HD	3H	HD8	***	0.30	2.23
HD	5H	HD16	***	0.22	1.58
HD	6H	HD17	***	0.26	1.84
HD	7H	HD18	***	0.27	1.95
HD	7H	HD21	***	0.40	3.17
HD	7H	HD22	*	0.21	1.47
					Total HD: 16.52
PH	1H	PH1	***	0.40	3.17
PH	2H	PH6	***	0.30	2.18
PH	2H	PH8	***	0.30	2.23
PH	3H	PH11	**	0.26	1.89
PH	3H	PH13	**	0.23	1.58
PH	3H	PH14	***	0.43	3.45
PH	4H	PH16	**	0.23	1.65
PH	4H	PH17	*	0.21	1.48
PH	5H	PH20	***	0.54	4.72
PH	5H	PH21	**	0.23	1.66
PH	6H	PH23	*	0.20	1.42
PH	7H	PH26	*	0.21	1.50
PH	7H	PH28	***	0.63	6.07
					Total PH: 32.99
TGW	1H	TGW3	*	0.18	1.22
TGW	2H	TGW5	**	0.23	1.63
TGW	4H	TGW14	***	0.39	3.02
TGW	5H	TGW15	***	0.32	2.40
TGW	5H	TGW16	*	0.20	1.36
TGW	5H	TGW18	***	0.26	1.85
TGW	6H	TGW20	*	0.18	1.23
TGW	7H	TGW26	***	0.32	2.41
TGW	7H	TGW27	**	0.21	1.50
					Total TGW: 16.61
GY	2H	GY2	***	0.57	5.08
GY	2H	GY4	**	0.20	1.41
GY	4H	GY6	.	0.16	1.08
GY	5H	GY7	***	0.30	2.23
GY	7H	GY9	***	0.26	1.86
GY	7H	GY10	*	0.18	1.22
GY	7H	GY11	***	0.39	3.00
					Total GY: 15.88

Table 5. Best candidate genes found for selected QTLs.

Trait	QTL	CHR	Candidate gene	Gene model ID	MorexV3 Annotation
HD	HD1	1H	WNK3	HORVU.MOREX.r3.1HG0004150	Kinase family protein
HD	HD2	1H	HvCMF10	HORVU.MOREX.r3.1HG0041150	Zinc finger protein CONSTANS
HD	HD3	1H	HvCO9	HORVU.MOREX.r3.1HG0058180	CONSTANS-like protein
HD	HD5	2H	HvCO18	HORVU.MOREX.r3.2HG0115000	CONSTANS-like protein
HD	HD9	3H	HvFDL-H4	HORVU.MOREX.r3.3HG0296180	BZIP transcription factor
HD	HD16	5H	HvFRI	HORVU.MOREX.r3.5HG0534990	FRIGIDA-like protein, putative
HD	HD17	6H	HvNUP160	HORVU.MOREX.r3.6HG0557980	Nuclear pore complex protein Nup 160
HD	HD21	7H	HvMADS26	HORVU.MOREX.r3.7HG0705340	MADS-box transcription factor
HD	HD22	7H	HvNF-Yb2	HORVU.MOREX.r3.7HG0734470	Nuclear transcription factor Y subunit B
PH	PH1	1H	HvNRT	HORVU.MOREX.r3.1HG0005090	Nitrate transporter 1.1
PH	PH3	1H	OsCKX9	HORVU.MOREX.r3.1HG0059670	Cytokinin oxidase/dehydrogenase
PH	PH4	1H	HvGA20x8a	HORVU.MOREX.r3.1HG0087020	Gibberellin 2-oxidase
PH	PH13	3H	OsWRKY21	HORVU.MOREX.r3.3HG0297540	WRKY transcription factor
PH	PH14	3H	HvGA20ox2 (sdw1/denso)	HORVU.MOREX.r3.3HG0297550	Gibberellin 20 oxidase
PH	PH20	5H	OsPH9	HORVU.MOREX.r3.5HG0496220	Histone H4
PH	PH24	6H	HvLAZY1	HORVU.MOREX.r3.6HG0632820	WRKY transcription factor-like protein
PH	PH29	7H	OsMYB45	HORVU.MOREX.r3.7HG0736780	Homeodomain-like superfamily protein
PH	PH29	7H	OsMYB45	HORVU.MOREX.r3.7HG0736790	Homeodomain-like superfamily protein
PH	PH29	7H	OsMYB45	HORVU.MOREX.r3.7HG0736800	Two-component response regulator
PH	PH29	7H	OsMYB45	HORVU.MOREX.r3.7HG0736840	MYB transcription factor-like
TGW	TGW2	1H	OsCKX9	HORVU.MOREX.r3.1HG0059670	Cytokinin oxidase/dehydrogenase
TGW	TGW2	1H	HvSMOS1	HORVU.MOREX.r3.1HG0058550	AP2-like ethylene-responsive transcription factor
TGW	TGW7	3H	HvRA2 (vrs4)	HORVU.MOREX.r3.3HG0233930	LOB domain protein
TGW	TGW8	3H	HvBRI1	HORVU.MOREX.r3.3HG0285210	Receptor kinase
TGW	TGW13	4H	HvGT1	HORVU.MOREX.r3.4HG0399240	Homeobox protein, putative
TGW	TGW14	4H	HvCMF4	HORVU.MOREX.r3.4HG0411680	Zinc finger protein CONSTANS
TGW	TGW18	5H	HvBRXL4	HORVU.MOREX.r3.5HG0535760	Protein BREVIS RADIX
TGW	TGW27	7H	HvJMJ	HORVU.MOREX.r3.7HG0752360	Lysine-specific demethylase
GY	GY1	1H	HvGA20x8a	HORVU.MOREX.r3.1HG0087020	Gibberellin 2-oxidase
GY	GY2	2H	HvHOX1	HORVU.MOREX.r3.2HG0184740	Homeobox leucine zipper protein
GY	GY5	3H	HvAGL2	HORVU.MOREX.r3.3HG0221900	Alpha-glucosidase
GY	GY8	7H	HvKAO1	HORVU.MOREX.r3.7HG0637750	Cytochrome P450
GY	GY11	7H	OsMYB45	HORVU.MOREX.r3.7HG0736780	Homeodomain-like superfamily protein
GY	GY11	7H	OsMYB45	HORVU.MOREX.r3.7HG0736790	Homeodomain-like superfamily protein
GY	GY11	7H	OsMYB45	HORVU.MOREX.r3.7HG0736800	Two-component response regulator
GY	GY11	7H	OsMYB45	HORVU.MOREX.r3.7HG0736840	MYB transcription factor-like

Figure legends

Figure 1. Plot of first two principal components of the AMMI analysis for heading date (Z55) of 151 spring two-rowed cultivars over 16 field trials.

Figure 2. Manhattan plot of the meta-analysis of 14 trials for grain yield (GY). In blue, threshold commonly used in meta-analyses in the literature. In red, threshold calculated in this study, corresponding to the minimum P-value resulting from 1000 permutations.

Figure 3. Allelic boxplots for four QTL (one for each trait), across environments. A) QTL HD5, days from sowing to heading, divided into autumn (left panel) and winter-spring sowings (right panel); B) QTL PH14, plant height; C) QTL TGW18, thousand grain weight; D) QTL GY2, grain yield.

Figure 4. Phenotype boxplots of all trials divided by groups of release years. A) Days from sowing to heading, B) plant height, C) thousand grain weight and D) grain yield.

Figure 5. Changes in allele frequencies of the QTLs identified in the meta-analyses for plant height (A) and grain yield (B) across time of release of the cultivars.

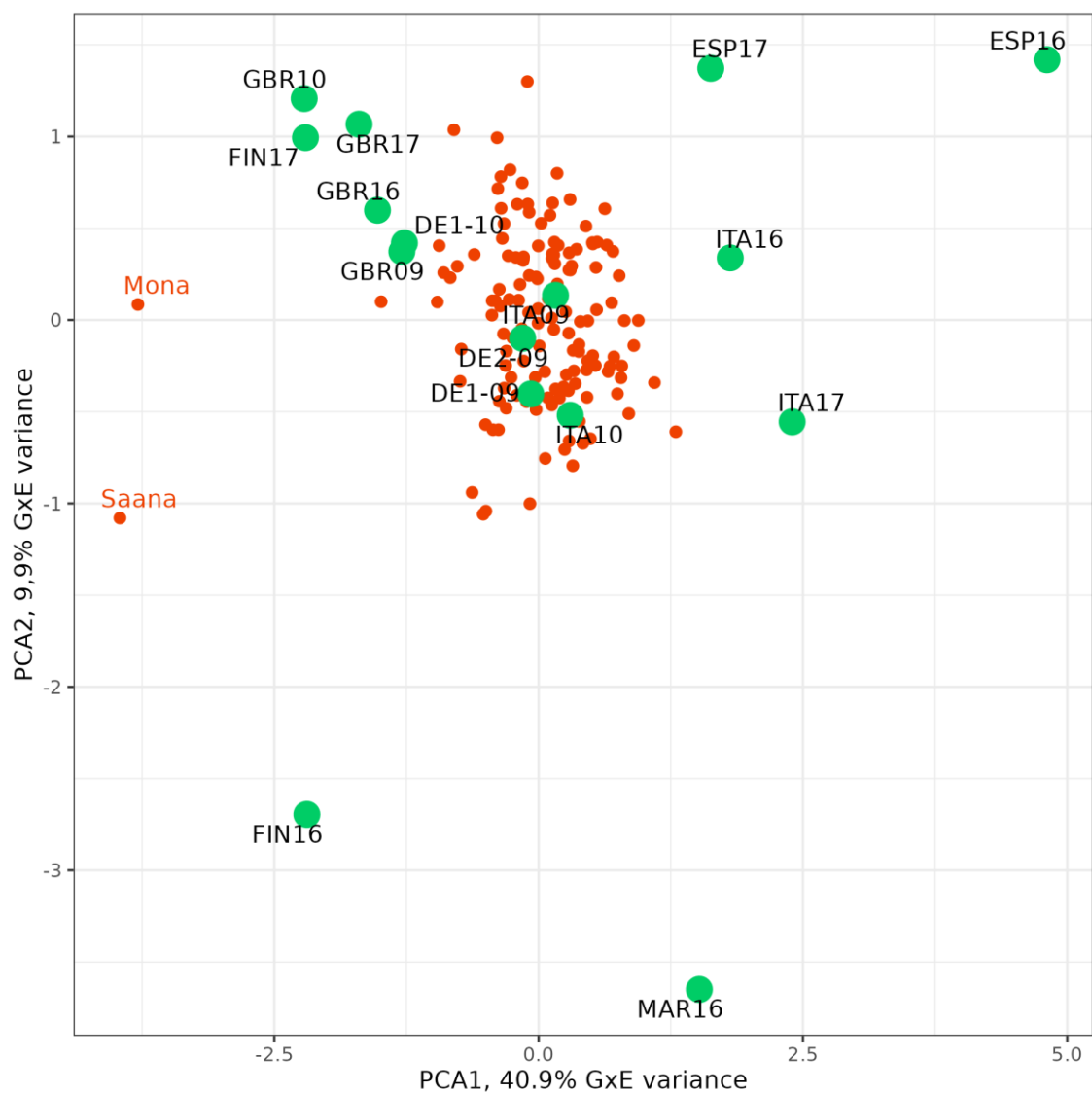


Figure 1. Plot of first two principal components of the AMMI analysis for heading date (Z55) of 151 spring two-rowed cultivars over 16 field trials.

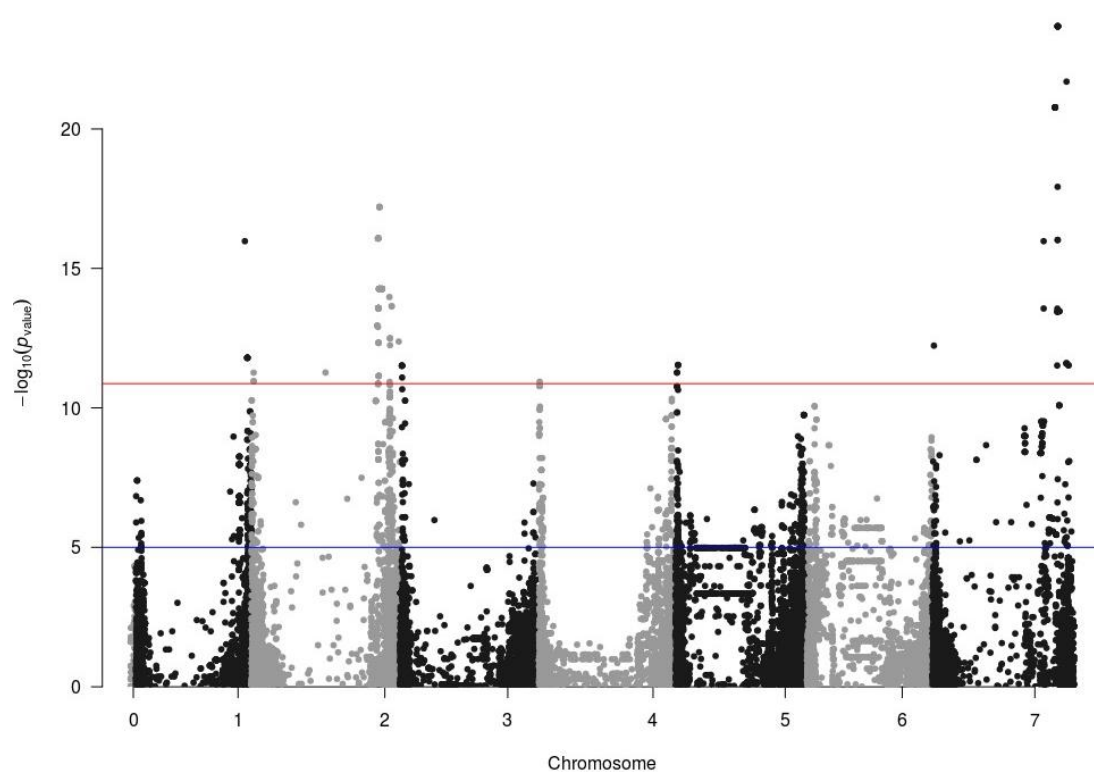
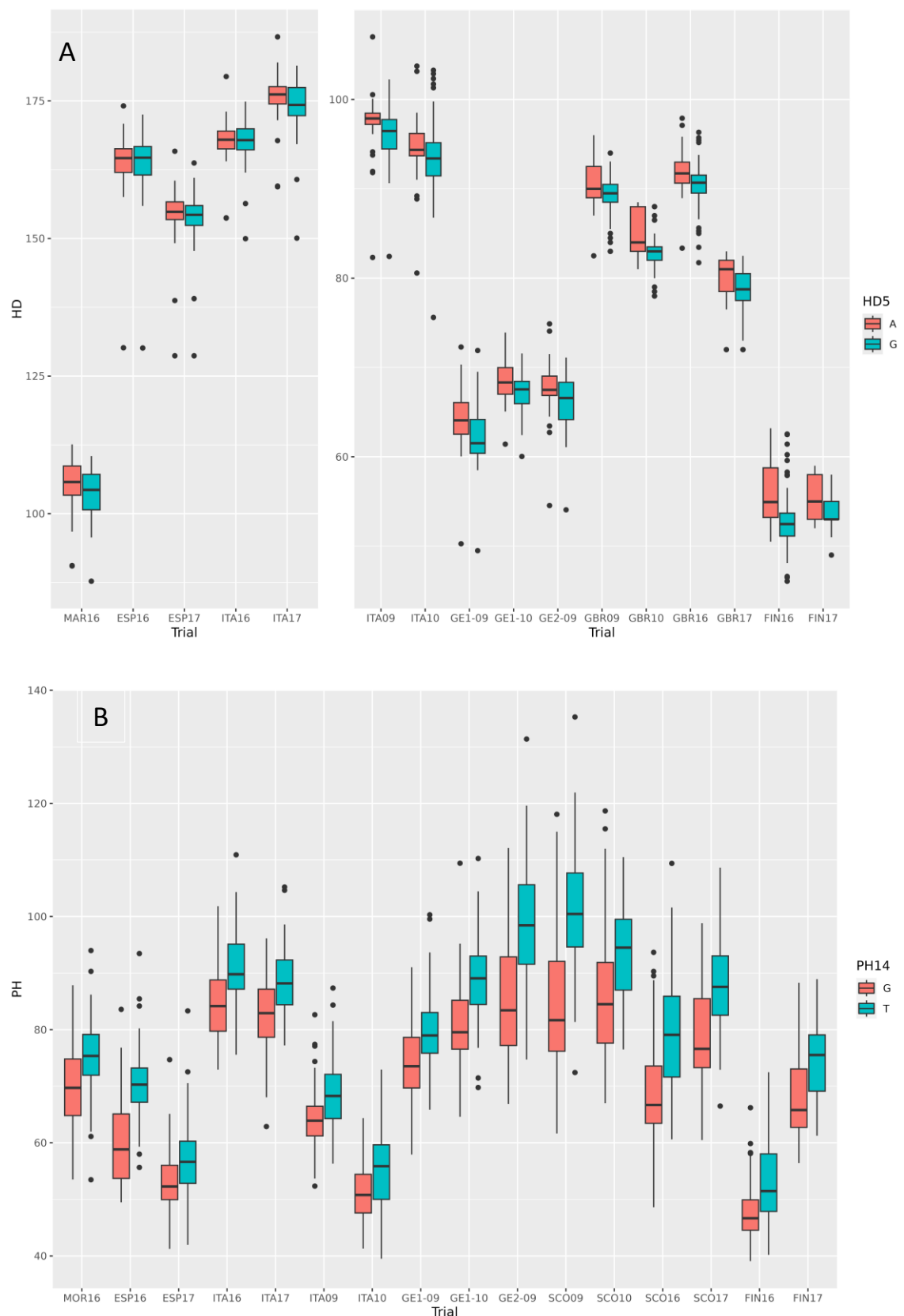


Figure 2. Manhattan plot of the meta-analysis of 14 trials for grain yield (GY). In blue, threshold commonly used in meta-analyses in the literature. In red, threshold calculated in this study, corresponding to the minimum P-value resulting from 1000 permutations.



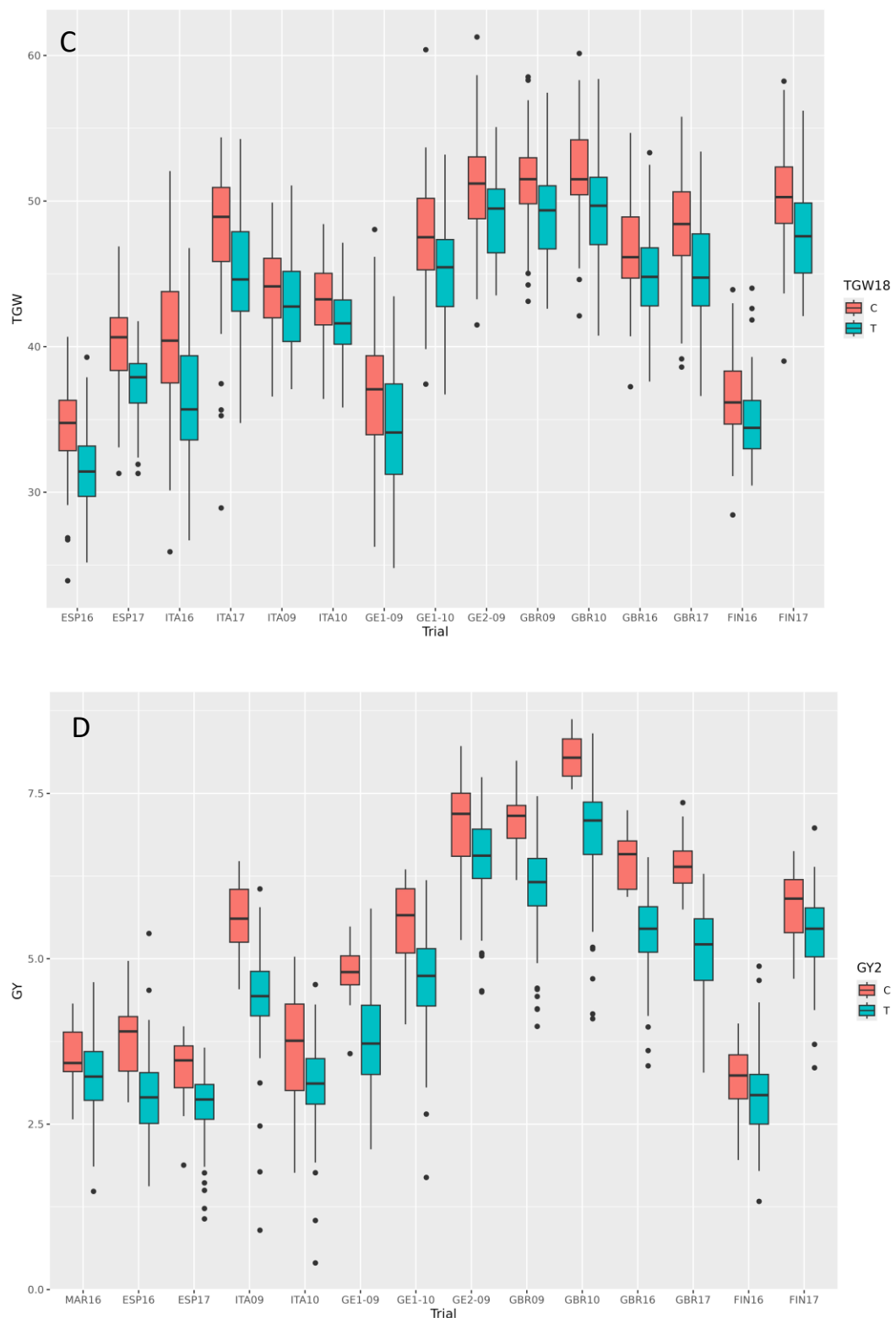


Figure 3. Allelic boxplots for four QTL (one for each trait), across environments. A) QTL HD5, days from sowing to heading, divided into autumn (left panel) and winter-spring sowings (right panel); B) QTL PH14, plant height; C) QTL TGW18, thousand grain weight; D) QTL GY2, grain yield.

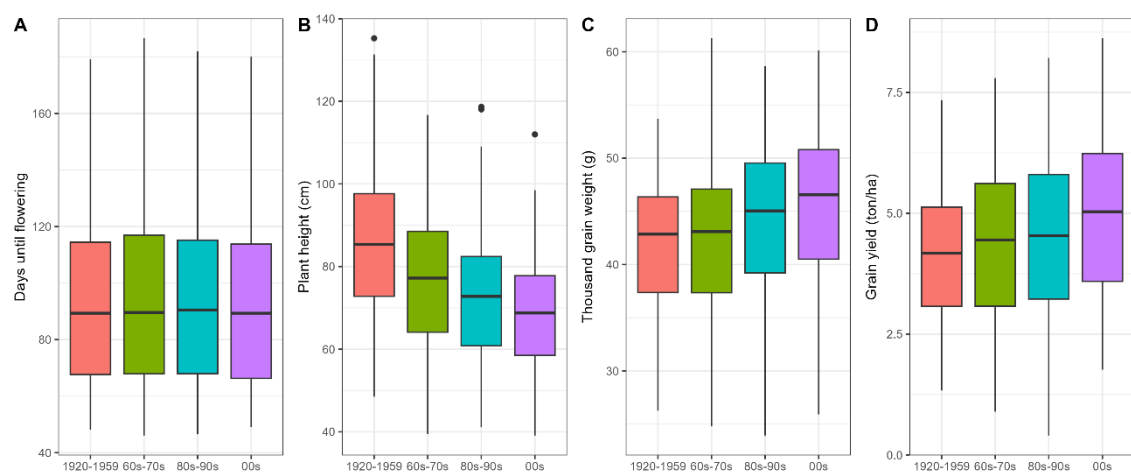


Figure 4. Phenotype boxplots of all trials divided by groups of release years. A) Days from sowing to heading, B) plant height, C) thousand grain weight and D) grain yield.

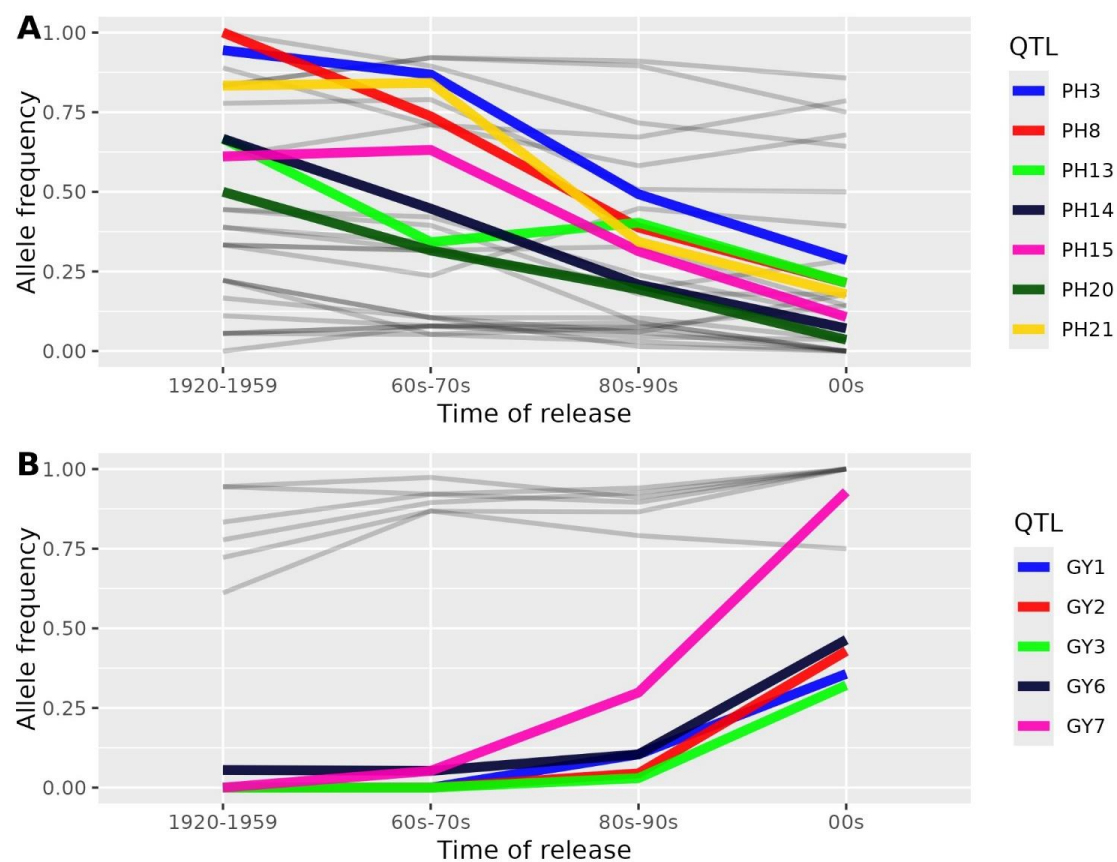


Figure 5. Changes in allele frequencies of the QTLs identified in the meta-analyses for plant height (A) and grain yield (B) across time of release of the cultivars.